

# **Application of the Wavelet Transform for Sparse Matrix Systems and PDEs**

by

**Issa Karambal**

Submitted in fulfilment of the academic requirements  
for the degree of Master of Science in the  
School of Mathematical Sciences  
University of KwaZulu-Natal  
Durban

Supervisor: Dr N.Parumasur

Co-supervisor: Dr P.Singh

March 26, 2009

# Abstract

We consider the application of the wavelet transform for solving sparse matrix systems and partial differential equations. The first part is devoted to the theory and algorithms of wavelets. The second part is concerned with the sparse representation of matrices and well-known operators. The third part is directed to the application of wavelets to partial differential equations, and to sparse linear systems resulting from differential equations. We present several numerical examples and simulations for the above cases.

# Preface

The work described in this dissertation was carried out in the School of Mathematical Sciences, University of KwaZulu-Natal, Durban, under the supervision of Dr N.Paramasur.

This study represents original work by the author and has not otherwise been submitted in any form for any degree or diploma to any other tertiary institution. Where use has been made of the work of others, it has been duly acknowledged in the text.

---

Issa Karambal

## Faculty of Science and Agriculture

### Declaration 1 - Plagiarism

I,....., declare that

1. The research reported in this thesis, except where otherwise indicated, is my original research.
2. This thesis has not been submitted for any degree or examination at any other university.
3. This thesis does not contain other persons data, pictures, graphs or other information, unless specifically acknowledged as being sourced from other persons.
4. This thesis does not contain other persons' writing, unless specifically acknowledged as being sourced from other researchers. Where other written sources have been quoted, then:
  - a. Their words have been re-written but the general information attributed to them has been referenced
  - b. Where their exact words have been used, then their writing has been placed in italics and inside quotation marks, and referenced.
5. This thesis does not contain text, graphics or tables copied and pasted from the Internet, unless specifically acknowledged, and the source being detailed in the thesis and in the References sections.

Signed \_\_\_\_\_

# Acknowledgments

I am very grateful to God for his goodness toward me, to my parents for their support, to AIMS (African Institute for Mathematical Sciences) for providing me funds, to Prof Jacek Banasiak for bringing me to UKZN, to my supervisor Dr N.Paramasur and my co supervisor Dr P.Singh for their help, to Dr Sergey Shindin for his advices on Matlab. Finally my gratitude extends to all my friends in particular Miranda Asah and Chama Abdulkadri.

# Contents

<b>List of Figures</b>	<b>viii</b>
<b>1 Introduction</b>	<b>1</b>
<b>2 Introduction to Wavelets</b>	<b>4</b>
2.1 Function spaces and other preliminaries . . . . .	4
2.2 Multiresolution analysis . . . . .	5
2.2.1 Compactly supported wavelets . . . . .	13
2.2.2 Decomposition algorithm . . . . .	18
2.2.3 Reconstruction algorithm . . . . .	19
2.3 Wavelets in two dimensions . . . . .	22
2.4 Biorthogonal wavelets . . . . .	23
2.5 Multiresolution on the interval . . . . .	24
<b>3 Representation of operators in wavelet basis</b>	<b>26</b>
3.1 The standard form . . . . .	26
3.2 The Non-standard form . . . . .	30
3.3 Non-Standard form representation of the operator $\frac{d^p}{dx^p}$ . . . . .	33
3.4 The NS-form of operator functions . . . . .	36
3.5 Examples of Representation of operators . . . . .	39
<b>4 Wavelets in Linear Algebra</b>	<b>44</b>
4.1 The Inverse Operator in Wavelet Basis . . . . .	44

4.2	Numerical examples . . . . .	49
<b>5</b>	<b>Ordinary Differential Equations</b>	<b>54</b>
5.1	The Weighted Residuals Method . . . . .	54
5.1.1	Galerkin's Method . . . . .	55
5.1.2	The Collocation Method . . . . .	55
5.2	Wavelet Galerkin Method . . . . .	56
5.3	Wavelet Collocation Method . . . . .	60
5.4	Numerical Results . . . . .	62
5.4.1	Amaratunga <i>et al.</i> Method . . . . .	62
5.4.2	Collocation Method (Bertoluzza's Method) . . . . .	63
<b>6</b>	<b>Partial Differential equations</b>	<b>67</b>
6.1	Numerical Quadrature . . . . .	67
6.2	Evaluating Functions in Wavelet Bases . . . . .	70
6.3	Numerical Results . . . . .	74
<b>7</b>	<b>Conclusion</b>	<b>78</b>
	<b>Bibliography</b>	<b>81</b>

# List of Figures

2.1	Haar scaling function and mother wavelet. . . . .	10
2.2	The norm of the error . . . . .	11
2.3	The function $\sin(2\pi t)$ on the top left and its projections into the subspaces $V_{-1}$ , $V_{-4}$ , $V_{-5}$ and $V_{-8}$ . . . . .	12
2.4	Daubechies scaling function and mother wavelet. . . . .	17
2.5	The wavelet decomposition algorithm. . . . .	19
2.6	The wavelet reconstruction algorithm. . . . .	20
2.7	The coefficients $\{s_k^j : k \in \mathbb{Z}\}$ and $\{d_k^j : k \in \mathbb{Z}\}$ at level $j = -9$ . . . . .	22
3.1	Organization of a matrix in the standard form. . . . .	30
3.2	Organization of the non-standard form of a matrix. Blanks denote zero entries. . . . .	32
3.3	The non-standard form of $\frac{d^2}{dx^2}$ . . . . .	40
3.4	The Non-standard form of the Example 3.2 . . . . .	41
3.5	The standard form of the Example 3.2 . . . . .	42
3.6	The Non-standard form of the Example 3.3 . . . . .	43
4.1	Condition numbers of the periodized matrix $L_p$ . "db6" denotes Daubechies wavelet with six vanishing moments. . . . .	48
4.2	Sparsity pattern of the matrix $\mathbf{B}$ obtained by using 'db3' and setting to zero entries with the absolute value less than $10^{-14}$ . . . . .	51
4.3	Sparsity pattern of the matrix $\mathbf{B}^{-1}$ computing via the iterative algorithm, entries with the absolute value greater than $10^{-9}$ are shown in blue. . . . .	52



4.4	Sparsity pattern of the matrix $(\mathbf{L}^w)^{-1}$ computing via the iterative algorithm, entries with the absolute value greater than $10^{-8}$ are shown in blue. . . . .	53
5.1	$\log_2$ of norm-2 error of Amaratunga method and FDM. . . . .	62
5.2	Exact and approximate solution . . . . .	63
5.3	Exact and approximate solution . . . . .	64
5.4	The exact and the approximate solution computed at scale $m = -4$ . . . . .	66
6.1	The solution of problem (6.42) with initial condition given in (6.43) computed using Crank-Nicolson scheme for several values of time $t$ where $\Delta t = 2^{-8}$ . . . .	74
6.2	The solution of problem (6.42) with initial condition given in (6.43) computed in the wavelet domain for several values of time $t$ where $\Delta t = 2^{-8}$ . . . . .	75
6.3	The solution of the problem (6.42) with $u_0(x)$ given in (6.44) computed in the wavelet domain for several values of time $t$ where $\Delta t = 2^{-8}$ . . . . .	76
6.4	The norm-2 of the error. . . . .	76
6.5	Solution of the problem (6.46) computed at every four time step. . . . .	77

# 1. Introduction

Wavelets are as indicated by the name "small waves" that allow representation of functions in time-frequency domain. Nowadays, due to its advantages over the classical Fourier analysis, they have enjoyed a considerable success in many areas of science such as applied mathematics, pure mathematics, physics, and signal processing.

The first informal appearance of a wavelet according to its history was in 1910 in the thesis of Alfred Haar in which he produced a complete orthonormal basis for a Hilbert space. However the formal introduction of this subject began in the early 1980s with Jean Morlet's work, a French geophysicist. He used the French word *ondelette*, meaning "small wave". Soon it was transferred to English by translating "onde" into "wave", giving "wavelet".

In 1986 and 1987 respectively, wavelets have undergone remarkable advances due to the work of S.Mallat and Y.Meyer, who have shown that the orthonormal wavelet basis could be constructed systematically from a general formalism. This led to the invention of multiresolution analysis, by Ingrid Daubechies as well as her construction of orthonormal wavelets with compact support having some degree of smoothness. Note that nowadays the construction of wavelets differ according to the situation.

For some purposes, the wavelet  $\psi$  is chosen to belong either to the space  $L^1 \cap L^2$ , or to the space of  $r$ -regular functions such that the dilated and translated function defined by  $\psi_{j,k}(t) = 2^{-\frac{j}{2}}\psi(2^{-j}t - k)$  form a complete orthonormal base of  $L^2(\mathbb{R})$ . Such a base is well suited for the study of Calderón-Zygmund operators and is as well an unconditional base of  $L^p(\mathbb{R})$ ,  $1 < p < +\infty$ , Hardy space  $H^1$ , Sobolev space  $W^{s,p}$ ,  $s \in \mathbb{R}$ , and Besov space in particular (see [24]).

Wavelet methods provide efficient algorithms to solve partial differential equations in the sense that the set of approximations to which the computed solution belongs must be close to the exact solution  $u$ , and the computation of the solution needs to be fast, that is, less time-consuming. Indeed, the good localization properties that wavelets display both in space and frequency are important to build such an algorithm. The vanishing moments property that wavelets possess is also very important for the numerical solution of PDE's, since only few wavelet coefficients are needed to represent the solution in a smooth region unlike the non smooth region, where a

---

significant number of wavelet coefficients are used.

The numerical methods applied for solving differential equations such as the finite difference or the finite element method lead generally to a sparse matrix with a large condition number which is not acceptable since it requires several iterations to obtain the solution. This happens if one uses an iterative method or a significant number of operations if one use the direct method (matrix-vector multiplication). We recall that the condition number controls the rate of convergence of a number of iterative algorithms for solving linear systems. However, it has been shown in [2] that by projecting the linear systems into the wavelet domain and rescaling it by a diagonal preconditioned matrix, we are guaranteed to obtain a small condition number, hence the solution is obtained in just a few iterations. For example, the number of iterations used to solve a linear system by the conjugate gradient method is proportional to  $O\left(\frac{\sqrt{\kappa}-1}{\sqrt{\kappa}+1}\right)$ , where  $\kappa$  is the condition number of the corresponding matrix. In wavelet bases, the inverse of the matrix obtained after discretization is sparse unlike in the ordinary domain. Therefore, we may take advantage of this, to construct it numerically.

The next chapter provides a brief introduction to wavelets with emphasis on compactly supported wavelets due to its relevancy to our future discussion. In Chapter 3, we consider the representations of operators in bases of compactly supported wavelets. For wide classes of operators, namely Calderón-Zygmund and pseudo-differential operators, it has been shown that they admit a sparse representation. The representation of these operators in wavelet bases is accomplished by the so-called non-standard form or the standard form [3]. The remarkable feature of the non-standard form is the uncoupling achieved among the scales, which results in a more sparse representation of the operator. On the other hand, the representation using the standard form results in a "finger-like" pattern, which is a consequence of the interaction between scales. We represent the differential operator and the operator function in the wavelet domain using the non-standard form. Chapter 4 is dedicated to the application of wavelets in linear algebra. As mentioned earlier, by projecting the sparse linear systems obtained after discretizing the partial differential equations and applying the diagonal preconditioner produces a well-conditioned system. Hence, wavelet bases may be viewed as fast solvers for PDE's. Our main focus in Chapters 5 and 6 is to use wavelet bases to solve differential equations. In Chapters 5, we are particularly interested in ordinary differential equations. We begin with Galerkin's method developed by Amaratunga *et al.*

---

[29] for solving differential equations of the Helmholtz type, where the dilates and translates of the scaling function  $\varphi$  is chosen to be the *test function*. In [29], the original problem is transformed to a convolution problem so that the transformation from the wavelet space to the physical space (or vice versa) may be easily accomplished using the FFT (Fast Fourier Transform). Next, we discuss wavelet collocation method as described in [1] for the equation of the form  $\mathcal{L}u = f$ , where  $\mathcal{L}$  is a linear differential operator. In this case, the authors have used the autocorrelation function  $\phi$  generated by the scaling function  $\varphi$  as the basis function to approximate the solution. Chapter 6 is focused on the numerical solution of the evolution equations where Beylkin *et al.* method is adopted.

## 2. Introduction to Wavelets

### 2.1 Function spaces and other preliminaries

We recall some spaces that are important in this thesis.

Let  $L^2$  be the Hilbert space of square-integrable functions defined by

$$L^2(\mathbb{R}) = \left\{ f : \mathbb{R} \rightarrow \mathbb{R} \text{ measurable} : \|f\|_2^2 = \int_{\mathbb{R}} |f(t)|^2 dt < +\infty \right\}$$

with the inner-product

$$\langle f, g \rangle = \int_{\mathbb{R}} f(t) \overline{g(t)} dt,$$

where the symbol  $\bar{\phantom{x}}$  denotes the complex conjugate. It is a complete and separable space.

Likewise, the *sequence space*  $l^2(\mathbb{Z})$  is defined by

$$l^2(\mathbb{Z}) = \left\{ c : \mathbb{Z} \rightarrow \mathbb{Z} : \|c\|_2^2 = \sum_{n \in \mathbb{Z}} |c_n|^2 < +\infty \right\}$$

Then we have some relevant inequalities that might be useful.

The *Cauchy-Schwartz's* inequality is given by

$$|\langle f, g \rangle| \leq \|f\|_2 \|g\|_2,$$

and the *triangle inequality* is defined as

$$\|f + g\|_2 \leq \|f\|_2 + \|g\|_2.$$

In an analogous manner we define  $L^2(0, 1)$ .

We say two functions  $f, g$  are *orthogonal*, and write  $f \perp g$  when  $\langle f, g \rangle = 0$ .

A sequence of functions  $\{f_n\}_{n \in \mathbb{N}}$  is an *orthonormal* sequence if  $\langle f_m, f_n \rangle = \delta_{m,n}$ , where  $\delta$  is the *symbol of Kronecker delta* defined by

$$\delta_{i,j} = \begin{cases} 1 & \text{if } i = j, \\ 0 & \text{otherwise.} \end{cases}$$

Let  $\mathcal{F}(f) = \hat{f}$  denote the Fourier transform of a function  $f \in L^1(\mathbb{R})$  defined by

$$\hat{f}(\xi) = \int_{\mathbb{R}} f(t)e^{-i\xi t} dt, \quad \xi \in \mathbb{R},$$

then the inversion formula can be written as

$$f(t) = \frac{1}{2\pi} \int_{\mathbb{R}} \hat{f}(\xi)e^{i\xi t} d\xi.$$

We therefore have the following property

$$\mathcal{F}(f(t - n)) = e^{-i\xi n} \hat{f}(\xi). \quad (2.1)$$

If  $f \in L^1(\mathbb{R}) \cap L^2(\mathbb{R})$  then  $\hat{f} \in L^2(\mathbb{R})$  and Plancherel's formula

$$\int_{\mathbb{R}} |f(t)|^2 dt = \frac{1}{2\pi} \int_{\mathbb{R}} |\hat{f}(\xi)|^2 d\xi \quad (2.2)$$

is valid.

The Plancherel's formula (2.2) implies Parseval's formula

$$\int_{\mathbb{R}} f(t)\overline{g(t)} dt = \frac{1}{2\pi} \int_{\mathbb{R}} \hat{f}(\xi)\overline{\hat{g}(\xi)} d\xi, \quad f, g \in L^2(\mathbb{R}). \quad (2.3)$$

## 2.2 Multiresolution analysis

Multiresolution analysis as introduced by Meyer and Mallat [22], is the decomposition of a function in  $L^2(\mathbb{R})$  into different scales. Following the convention of decreasing subspaces by Daubechies and Mallat [16], we now give the definition of the *multiresolution analysis*.

**Definition 2.1.** A sequence  $(V_j)_{j \in \mathbb{Z}}$  of subspaces of  $L^2(\mathbb{R})$  is a MRA<sup>1</sup> if:

1. For all  $j \in \mathbb{Z}$ ,  $V_j \subset V_{j-1}$
2.  $\bigcap_{j \in \mathbb{Z}} V_j = \lim_{j \rightarrow +\infty} V_j = \{0\}$
3.  $\overline{\bigcup_{j \in \mathbb{Z}} V_j} = \lim_{j \rightarrow -\infty} V_j = L^2(\mathbb{R})$

---

<sup>1</sup>Multiresolution analysis

4. For any  $f \in L^2(\mathbb{R})$  and any  $k \in \mathbb{Z}$ ,  $f(t) \in V_0$  if and only if  $f(t - k) \in V_0$
5. For any  $f \in L^2(\mathbb{R})$  and any  $j \in \mathbb{Z}$ ,  $f(t) \in V_j$  if and only if  $f(2t) \in V_{j-1}$
6. There exists a function  $\varphi \in V_0$  called the *scaling function*, such that the system  $\{\varphi(t - k)\}_{k \in \mathbb{Z}}$  is a Riesz basis of  $V_0$ .

Notation:  $\sum_{k \in \mathbb{Z}}$  will be denoted by  $\sum_k$  in the future

Before making an observation related to the Definition 2.1, let us recall that a family of functions  $\{\varphi(t - k), k \in \mathbb{Z}\}$  is a Riesz basis of  $V_0$ , if there exists  $A$  and  $B$ ,  $B \geq A > 0$  that satisfy

$$A \sum_k |s_k|^2 \leq \int_{\mathbb{R}} \left| \sum_k s_k \varphi_k \right|^2 dt \leq B \sum_k |s_k|^2,$$

and  $\text{span}\{\varphi(t - k), k \in \mathbb{Z}\} = V_0$ .

**Remark 2.1.** If  $A = B = 1$ , we obtain an orthonormal basis.

Conditions 1 to 3 mean that every function in  $L^2(\mathbb{R})$  can be well approximated by elements of the subspaces  $V_j$ , and as  $j$  approaches  $-\infty$ , the precision of approximation increases. Condition 4 expresses the invariance of the subspace  $V_0$  with respect to the translation.

Let the dilated and translated function  $\varphi_{j,k}$  be defined by

$$\varphi_{j,k}(t) = 2^{-\frac{j}{2}} \varphi(2^{-j}t - k). \quad (2.4)$$

Then according to Definition 2.1, the system  $\{\varphi_{j,k}, k \in \mathbb{Z}\}$  is an orthonormal basis of  $V_j$ .

Since  $\varphi \in V_0 \subset V_{-1}$ , and the  $\varphi_{-1,k}$  are an orthonormal basis in  $V_{-1}$ , there exists a sequence  $(h_k)_{k \in \mathbb{Z}} \in l^2(\mathbb{Z})$  called *filter coefficients* such that the scaling function satisfies

$$\varphi(t) = \sqrt{2} \sum_k h_k \varphi(2t - k), \quad (2.5)$$

which is the well known *dilation equation* or *refinement equation*, and

$$\int_{\mathbb{R}} \varphi(t) dt = 1. \quad (2.6)$$

Let  $W_j$  be the orthogonal complement of  $V_j$  in  $V_{j-1}$  i.e.

$$V_{j-1} = V_j \oplus W_j \quad (2.7)$$

where  $\oplus$  denotes a direct sum. Then there exists a function  $\psi \in W_0 \subset V_{-1}$  called the *mother wavelet* defined by

$$\psi(t) = \sqrt{2} \sum_k g_k \varphi(2t - k), \quad \text{where } g_k = (-1)^k h_{1-k}, \quad (2.8)$$

and satisfying

$$\int_{\mathbb{R}} \psi(t) dt = 0. \quad (2.9)$$

Similarly, the system  $\{\psi_{j,k}(t) = 2^{-\frac{j}{2}} \psi(2^{-j}t - k), \quad k \in \mathbb{Z}\}$  is an orthonormal basis of  $W_j$ .

Noting that for every  $j \in \mathbb{Z}$ ,  $W_j \subset V_{j-1}$  we get

$$L^2(\mathbb{R}) = \bigoplus_{j \in \mathbb{Z}} W_j, \quad (2.10)$$

and if there is the coarsest scale  $n$ , then (2.10) is replaced by

$$L^2(\mathbb{R}) = V_n \bigoplus_{j \leq n} W_j. \quad (2.11)$$

Let  $P_j$  and  $Q_j$  denote the orthogonal projection operators onto  $V_j$  and  $W_j$ , respectively. Then any function  $f \in L^2(\mathbb{R})$  projected onto  $V_{j-1}$  may be expressed as (see 2.7)

$$P_{j-1}f = P_j f + Q_j f, \quad (2.12)$$

where

$$P_j f = \sum_k \langle f, \varphi_{j,k} \rangle \varphi_{j,k} = \sum_k s_k^j \varphi_{j,k}, \quad (2.13)$$

and

$$Q_j f = \sum_k \langle f, \psi_{j,k} \rangle \psi_{j,k} = \sum_k d_k^j \psi_{j,k} \quad (2.14)$$

are respectively the approximation and the error of  $f$  at the resolution level  $j$ .

Thus if our coarse subspace is  $V_0$  then according to (2.11),  $f$  can be written as

$$f(t) = \sum_k s_k^0 \varphi(t - k) + \sum_j \sum_k 2^{-j/2} d_k^j \psi(2^{-j}t - k). \quad (2.15)$$

**Lemma 2.1.** [16] *For all continuous functions  $f \in L^2(\mathbb{R})$ ,*

$$\lim_{j \rightarrow -\infty} \|P_j(f) - f\|_{L^2} = 0, \quad (2.16)$$

and

$$\lim_{j \rightarrow +\infty} \|P_j(f)\|_{L^2} = 0.$$



*Proof.* Since  $\bigcup_{j \in \mathbb{Z}} V_j$  is dense in  $L^2(\mathbb{R})$ , then for  $\epsilon > 0$  there exists  $k \in \mathbb{Z}$  and  $u(t) \in V_k$  such that  $\|f - u\|_{L^2} < \epsilon/2$ . By Definition 2.1(1),  $u(t) \in V_j$  and  $P_j u(t) = u(t)$  for all  $k \geq j$ . Thus by the triangle inequality we have

$$\begin{aligned} \|f - P_j f\|_{L^2} &= \|f - u + P_j u - P_j f\|_{L^2}, \\ &\leq \|f - u\|_{L^2} + \|P_j(f - u)\|_{L^2}, \\ &= 2\|f - u\|_{L^2} < \epsilon, \quad (f - u) \in W_k \subset V_j. \end{aligned}$$

Hence,

$$\|f - P_j f\|_{L^2} < \epsilon.$$

Since this inequality holds for all  $k \geq j$ , we get  $\lim_{j \rightarrow -\infty} \|P_j(f) - f\|_{L^2} = 0$ .

Notation:  $\text{supp}(f)$  denotes support of  $f$ .

We now prove the second equality. Let us suppose that  $\text{supp}(f) \subset [-R, R]$  and let  $\epsilon > 0$ .

As  $\{\varphi_{j,k}\}_{k \in \mathbb{Z}}$  is an orthonormal basis in  $V_j$ , we have by applying the Cauchy-Schwartz inequality

$$\begin{aligned} \|P_j f\|_{L^2}^2 &= \sum_k |\langle P_j f, \varphi_{j,k} \rangle|^2 \\ &= \sum_k |\langle f, \varphi_{j,k} \rangle|^2 \\ &= \sum_k \left| \int_{-R}^R f(t) 2^{-j/2} \varphi(2^{-j}t - k) dt \right|^2, \\ &\leq \sum_k \left( \int_{-R}^R |f(t)|^2 dt \right) 2^{-j} \left( \int_{-R}^R |\varphi(2^{-j}t - k)|^2 dt \right), \\ &= \|f\|_{L^2}^2 \sum_k \int_{-2^{-j}R-k}^{2^{-j}R-k} |\varphi(x)|^2 dx. \end{aligned}$$

Observe that there exists a  $j_0 \in \mathbb{Z}$  such that for  $j > j_0$  we have  $2^{-j}R < \frac{1}{2}$ . Therefore

$$\sum_k \int_{-2^{-j}R-k}^{2^{-j}R-k} |\varphi(x)|^2 dx \leq \sum_k \int_{-\frac{1}{2}-k}^{\frac{1}{2}-k} |\varphi(x)|^2 dx.$$

If we choose  $K$  so large then

$$\sum_{|k| > K} \int_{-2^{-j}R-k}^{2^{-j}R-k} |\varphi(x)|^2 dx \leq \sum_{|k| > K} \int_{-\frac{1}{2}-k}^{\frac{1}{2}-k} |\varphi(x)|^2 dx = \int_{|x| \geq K - \frac{1}{2}} |\varphi(x)|^2 dx \leq \epsilon.$$

Since for each  $k \in \mathbb{Z}$ , we have

$$\lim_{j \rightarrow \infty} \int_{-2^{-j}R-k}^{2^{-j}R-k} |\varphi(x)|^2 dx = 0.$$

Hence

$$\begin{aligned} \lim_{j \rightarrow \infty} \|P_j f\|_{L^2}^2 &\leq \|f\|_{L^2}^2 \lim_{j \rightarrow \infty} \sum_k \int_{-2^{-j}R-k}^{2^{-j}R-k} |\varphi(x)|^2 dx, \\ &= \|f\|_{L^2}^2 \lim_{j \rightarrow \infty} \left( \sum_{|k| \leq K} \int_{-2^{-j}R-k}^{2^{-j}R-k} |\varphi(x)|^2 dx + \sum_{|k| > K} \int_{-2^{-j}R-k}^{2^{-j}R-k} |\varphi(x)|^2 dx \right), \\ &\leq \|f\|_{L^2}^2 \lim_{j \rightarrow \infty} \left( \sum_{|k| > K} \int_{-2^{-j}R-k}^{2^{-j}R-k} |\varphi(x)|^2 dx \right), \\ &= \|f\|_{L^2}^2 \epsilon. \end{aligned}$$

Since  $\epsilon > 0$  was arbitrary, the result follows.  $\square$

Note that Lemma 2.1 shows that condition 2 and 3 of the Definition 2.1 hold.

**Example 2.1.** (Haar Multiresolution)

The approximation of a function  $f \in L^2(\mathbb{R})$  by a piecewise constant function on the dyadic interval  $[2^j k, 2^j(k+1))$  is achieved by the MRA

$$V_j = \{g \in L^2(\mathbb{R}) : \forall k \in \mathbb{Z}, g|_{[2^j k, 2^j(k+1))} = \text{constant}\}, \quad (2.17)$$

where the symbol  $|_{[2^j k, 2^j(k+1))}$  denotes the restriction of  $g$  on the interval  $[2^j k, 2^j(k+1))$ .

The scaling function is defined by

$$\varphi(t) = \begin{cases} 1 & t \in [0, 1), \\ 0 & \text{elsewhere,} \end{cases} \quad (2.18)$$

and the mother wavelet by

$$\psi(t) = \begin{cases} 1 & t \in [0, \frac{1}{2}), \\ -1 & t \in [\frac{1}{2}, 1), \\ 0 & \text{elsewhere.} \end{cases}$$

It is clear that

$$\int_{\mathbb{R}} \psi(t) dt = 0,$$

and has the compact support  $[0, 1]$ .

The only disadvantage of the Haar wavelet is the discontinuities at the points  $\{0, \frac{1}{2}, 1\}$ , and in addition in practice we often deal with smooth functions ( particularly in image compressing), therefore we require a smooth wavelet, so the Haar wavelet is not appropriate in such a case.

Figure 2.1 illustrates the Haar scaling function and mother wavelet.

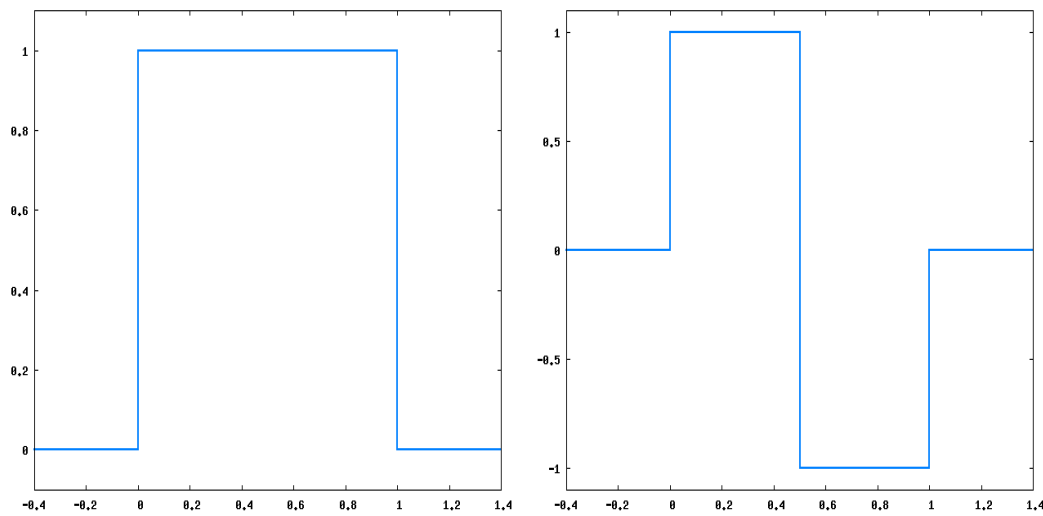


Figure 2.1: Haar scaling function and mother wavelet.

**Example 2.2.** To illustrate Lemma 2.1, we consider a smooth function defined by

$$\begin{aligned} f &: [0, 1] \longrightarrow \mathbb{R} \\ t &\longmapsto \sin(2\pi t). \end{aligned}$$

Using the multiresolution (2.17), we project  $f(t)$  into the subspace  $V_j$ , that is

$$f_j = P_j(f) = \sum_{k=0}^{2^{-j}-1} s_k^j \varphi_{j,k},$$

where  $\varphi$  is defined in (2.18).

We now compute the coefficients  $s_k^j$  defined by

$$s_k^j = \int_{\mathbb{R}} f(t) \varphi_{j,k}(t) dt. \quad (2.19)$$

Since  $\varphi_{j,k} = 2^{-j/2}$  on  $[2^j k, 2^j(k+1))$ , (2.19) becomes

$$\begin{aligned} s_k^j &= \int_{\mathbb{R}} f(t) \varphi_{j,k}(t) dt, \\ &= 2^{-j/2} \int_{2^j k}^{2^j(k+1)} \sin(2\pi t) dt, \\ &= -2^{-j/2} \frac{1}{2\pi} \cos(2\pi t) \Big|_{2^j k}^{2^j(k+1)}. \end{aligned}$$

Hence

$$s_k^j = 2^{-j/2} \frac{1}{2\pi} [\sin(2^j \pi(2k+1)) \sin(2^j \pi)], \quad j = 0, -1, -2, \dots$$

In Figure 2.2, we display the plot of the norm of the error (2.16). One can notice, as we decrease the resolution, that is  $j$  tends to  $-\infty$ , the norm of the error tends to zero which means that the approximation becomes better and better. Figure 2.3 shows the projection of the function  $f$  at different scales  $j$ .

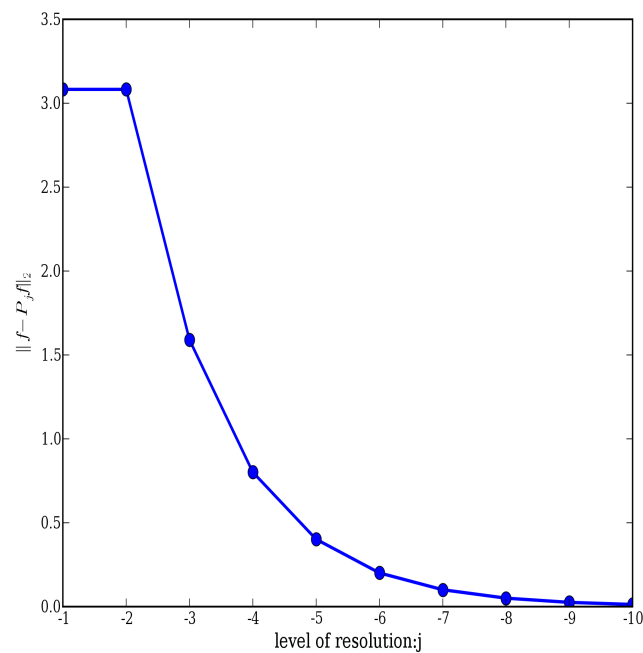


Figure 2.2: The norm of the error

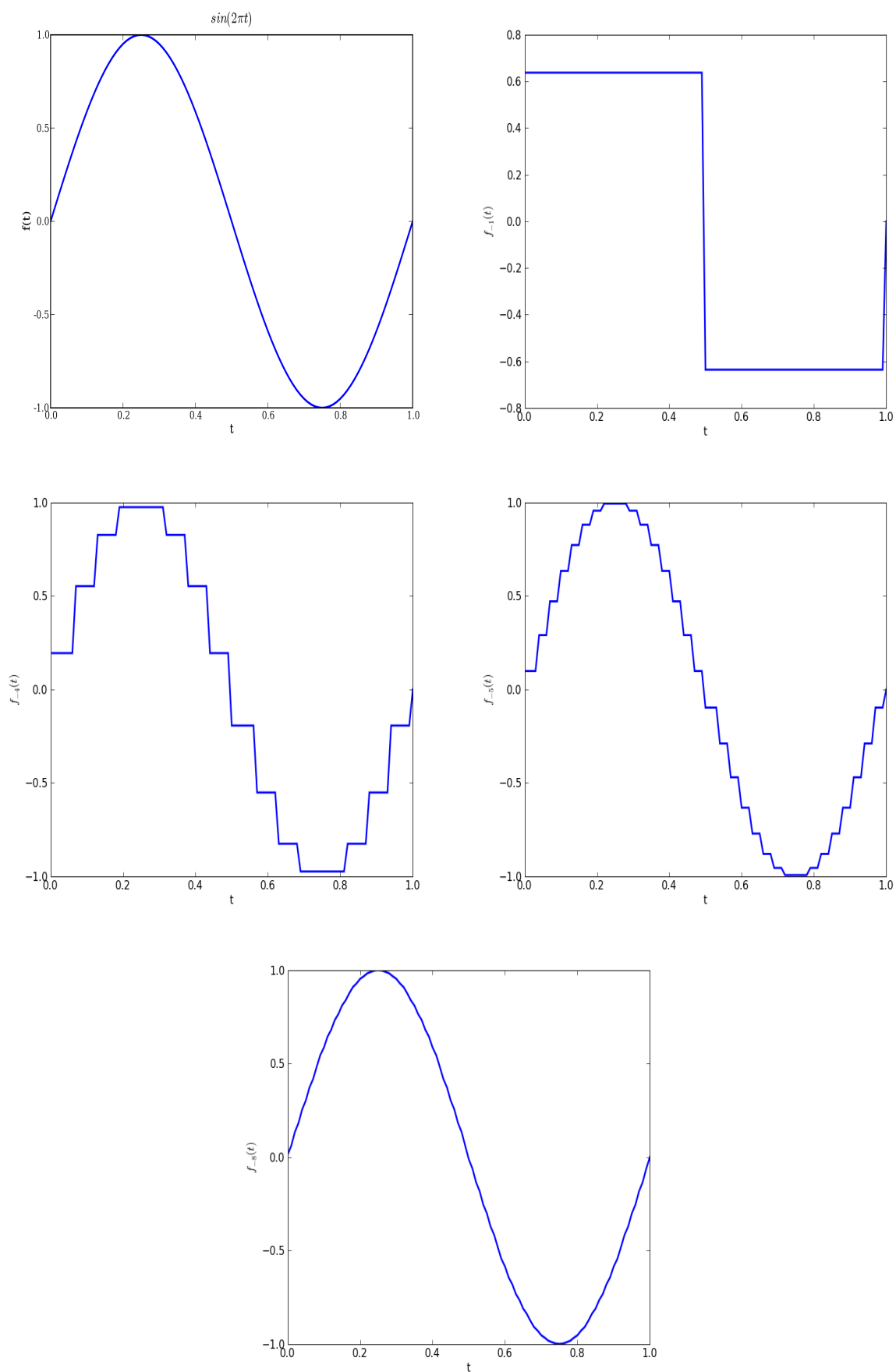


Figure 2.3: The function  $\sin(2\pi t)$  on the top left and its projections into the subspaces  $V_{-1}$ ,  $V_{-4}$ ,  $V_{-5}$  and  $V_{-8}$ .

**Remark 2.2.** Note that we can adopt two ways of looking at a MRA.

- We take the subspaces  $(V_j)_{j \in \mathbb{Z}}$  as our basic, given objects. They have to satisfy certain conditions which usually are rather easy to check. Then we need to find a scaling function satisfying (2.5). This is usually not so obvious.
- We start with the function  $\varphi$ . We define  $V_0$  as  $\text{span}\{\varphi(t - k)\}_{k \in \mathbb{Z}}$  and the other spaces  $V_j$  are defined by condition 5. Thereafter we need to check conditions 1-3 and 4 of the Definition 2.1.

**Remark 2.3.** We assume throughout this thesis that the mother wavelet  $\psi$  is  $M$  times differentiable and that its derivatives are continuous and rapidly decreasing. That is,  $\psi$  satisfies

$$|\psi^{(k)}(t)| \leq C_{p,k}(1 + |t|)^{-p}, \quad k = 0, 1, \dots, M - 1, \quad p \in \mathbb{Z}, \quad t \in \mathbb{R},$$

where  $C_{p,k}$  is a constant that depends on  $p$  and  $k$ .

### 2.2.1 Compactly supported wavelets

Here we introduce briefly I. Daubechies' approach [16] for the construction of orthonormal wavelets having compact support and some degree of smoothness. Indeed, this approach consists of seeking the *filter coefficients*  $\{h_k\}$  having compact support, that is

$$h_k = 0, \text{ for } k \notin \{0, 1, \dots, 2M - 1\} \quad (2.20)$$

such that the orthonormality condition is satisfied (see (2.24) below).

So (2.5) and (2.8) may be rewritten as

$$\begin{aligned} \varphi(t) &= \sqrt{2} \sum_{k=0}^{L-1} h_k \varphi(2t - k), \\ \psi(t) &= \sqrt{2} \sum_{k=0}^{L-1} g_k \varphi(2t - k), \end{aligned}$$

with  $L = 2M$  and

$$g_k = (-1)^k h_{L-k-1}, \quad k = 0, 1, \dots, L - 1. \quad (2.21)$$

In addition, we require that the wavelet  $\psi$  has  $M$  vanishing moments, that is

$$\int_{\mathbb{R}} t^m \psi(t) dt = 0, \quad m = 0, 1, \dots, M - 1. \quad (2.22)$$

The vanishing moments imply that every polynomial of degree  $M - 1$  may be represented as the linear combination of the scaling function in the subspace  $V_0$ .

Since  $\varphi(t)$  and  $\varphi(t - j)$  are orthonormal in  $V_0$ , and by Parseval's formula (2.3) and using (2.1), we have

$$\begin{aligned}
 \delta_{j,0} &= \int_{-\infty}^{\infty} \varphi(t)\varphi(t-j)dt = \int_{-\infty}^{\infty} \varphi(t)\overline{\varphi(t-j)}dt, \\
 &= \frac{1}{2\pi} \int_{-\infty}^{\infty} \hat{\varphi}(\xi)e^{i\xi j}\overline{\hat{\varphi}(\xi)}d\xi, \\
 &= \frac{1}{2\pi} \int_{-\infty}^{+\infty} |\hat{\varphi}(\xi)|^2 e^{i\xi j} d\xi, \\
 &= \frac{1}{2\pi} \int_0^{2\pi} \sum_k |\hat{\varphi}(\xi + 2\pi k)|^2 e^{i\xi j} d\xi, \\
 &= \frac{1}{2\pi} \int_0^{2\pi} \sum_k |\hat{\varphi}(\xi + 2\pi k)|^2 e^{i\xi j} d\xi.
 \end{aligned} \tag{2.23}$$

Hence the orthonormality condition in the frequency domain is given by

$$\sum_k |\hat{\varphi}(\xi + 2\pi k)|^2 = 1, \tag{2.24}$$

or in terms of the filter coefficients, (2.23) implies

$$\delta_{j,0} = \sum_{k=0}^{L-1} h_k h_{k-2j}, \quad \text{where } j \in \mathbb{Z}, \tag{2.25}$$

with

$$\sum_{k=0}^{L-1} h_k = \sqrt{2}.$$

Furthermore, transforming (2.5) into the Fourier domain, we have

$$\begin{aligned}
 \hat{\varphi}(\xi) &= \sqrt{2} \sum_k h_k \int_{\mathbb{R}} \varphi(2t - k)e^{-it\xi} dt, \\
 &= \frac{1}{\sqrt{2}} \sum_k h_k \int_{\mathbb{R}} \varphi(u)e^{-i\xi(\frac{u+k}{2})} du.
 \end{aligned}$$

Hence

$$\hat{\varphi}(\xi) = m_0(\xi/2)\hat{\varphi}(\xi/2), \tag{2.26}$$

where  $m_0$  is the function with period  $2\pi$  defined by

$$m_0(\xi) = \frac{1}{\sqrt{2}} \sum_{k=0}^{L-1} h_k e^{-ik\xi}. \tag{2.27}$$

Equations (2.26), (2.27) and (2.24) imply

$$|m_0(\xi)|^2 + |m_0(\xi + \pi)|^2 = 1. \quad (2.28)$$

We state the following result without proof.

**Proposition 2.1.** *A trigonometric polynomial  $m_0$  of the form [16]*

$$m_0(\xi) = \left( \frac{1 + e^{-i\xi}}{2} \right)^M \mathcal{L}(\xi) \quad (2.29)$$

*satisfies (2.28) if and only if  $L(\xi) = |\mathcal{L}(\xi)|^2$  can be written as*

$$L(\xi) = P(\sin^2 \xi/2),$$

*with*

$$P(y) = P_M(y) + y^M R\left(\frac{1}{2} - y\right),$$

*where*

$$P_M(y) = \sum_{k=0}^{M-1} \binom{M-1+k}{k} y^k$$

*and  $R$  is an odd polynomial chosen such that  $P(y) \geq 0$  for  $y \in [0, 1]$ .*

**Example 2.3.** In this example we compute the filter coefficients for  $M = 2$ .

From Proposition 2.1, we have that

$$\begin{aligned} P(y) &= 1 + 2y, \\ P(\sin^2 \xi/2) &= 2 - \cos(\xi). \end{aligned} \quad (2.30)$$

We seek a trigonometric polynomial  $\mathcal{L}$  of the form

$$\mathcal{L}(\xi) = a + be^{-i\xi}, \quad a, b \in \mathbb{R}. \quad (2.31)$$

We obtain

$$\begin{aligned} |\mathcal{L}(\xi)|^2 &= (a + be^{-i\xi})(a + be^{i\xi}), \\ &= (a^2 + b^2) + 2ab \cos(\xi). \end{aligned} \quad (2.32)$$

By matching coefficients in (2.32) and (2.30),

$$a^2 + b^2 = 2 \quad \text{and} \quad 2ab = -1,$$



so that

$$(a + b)^2 = a^2 + b^2 + 2ab = 1 \quad \text{and} \quad (a - b)^2 = a^2 + b^2 - 2ab = 3.$$

Equations (2.26), (2.29) and Lemma 2.2 imply  $m_0(0) = \mathcal{L}(0) = a + b = 1$ , so we have the linear system

$$\begin{cases} a + b = 1 \\ a - b = \pm\sqrt{3}. \end{cases} \quad (2.33)$$

Solving (2.33) gives either

$$a = \frac{1 + \sqrt{3}}{2}, \quad b = \frac{1 - \sqrt{3}}{2},$$

or vice versa.

Substituting the values of  $a$  and  $b$  in (2.31), and matching coefficients of (2.27) and (2.29), we have

$$h_0 = \frac{1 + \sqrt{3}}{4\sqrt{2}}, \quad h_1 = \frac{3 + \sqrt{3}}{4\sqrt{2}}, \quad h_2 = \frac{3 - \sqrt{3}}{4\sqrt{2}}, \quad h_3 = \frac{1 - \sqrt{3}}{4\sqrt{2}}.$$

In many cases there is no explicit expression for the scaling function  $\varphi$  (Daubechies wavelets), and therefore instead of working with the scaling function itself, we often use the filter coefficients  $h_k$ . However, the evaluation of  $\varphi$  may be accomplished by some well known approaches.

We may use the iteration approach which starts with the function  $\varphi^0(t)$  defined by

$$\varphi^0(t) = \begin{cases} 1 & t \in [0, 1), \\ 0 & \text{elsewhere,} \end{cases}$$

and iteratively define

$$\varphi^{n+1}(t) = \sqrt{2} \sum_k h_k \varphi^n(2t - k), \quad n \in \mathbb{N}.$$

If the iteration converges, the solution will be given by

$$\lim_{n \rightarrow \infty} \varphi^n(t).$$

This is known as the *cascade algorithm*.

Figure 2.4 is obtained by the above iteration method with  $n = 7$ ,  $M = 2$ .

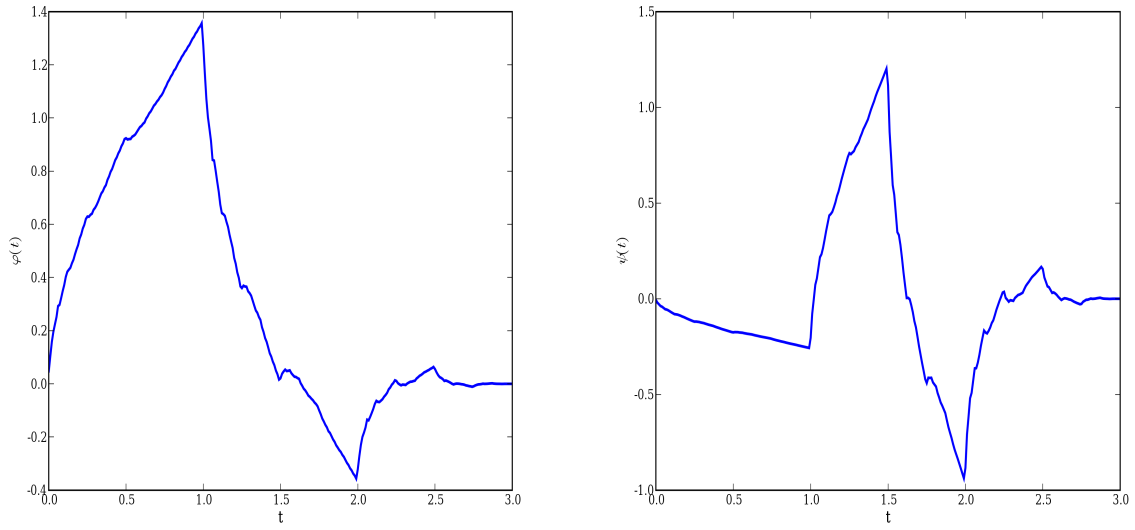


Figure 2.4: Daubechies scaling function and mother wavelet.

**Lemma 2.2.** Let  $\varphi$  be a scaling function of an MRA. Then

1.  $\hat{\varphi}(2\pi n) = 0$  for all integers  $n \neq 0$  and  $\hat{\varphi}(0) = 1$ ,
2.  $\sum_k \varphi(t - k) = 1$ .

*Proof.* Taking the Fourier transform of  $\varphi$ , setting  $\xi = 0$  and using (2.6), we have

$$\hat{\varphi}(0) = 1. \quad (2.34)$$

By setting again  $\xi = 0$  in (2.24), we have

$$\sum_n |\hat{\varphi}(2\pi n)|^2 = 1.$$

Since (2.34) is valid, we must have

$$\sum_{n \neq 0} |\hat{\varphi}(2\pi n)|^2 = 0.$$

Hence,  $\hat{\varphi}(2\pi n) = 0$  for  $n \neq 0$ .

2. Let  $\tilde{\varphi}(t) = \sum_n \varphi(t - n)$ .  $\tilde{\varphi}$  is periodic with period equal to 1, then we may write it in terms of a Fourier series expansion as

$$\tilde{\varphi}(t) = \sum_k c_k e^{i2\pi kt},$$

where

$$\begin{aligned}
 c_k &= \int_0^1 \tilde{\varphi}(t) e^{-i2\pi kt} dt, \\
 &= \int_0^1 \left( \sum_n \varphi(t-n) \right) e^{-i2\pi kt} dt, \\
 &= \sum_n \int_{-n}^{1-n} \varphi(t) e^{-i2\pi kt} dt, \\
 &= \int_{-\infty}^{\infty} \varphi(t) e^{-i2\pi kt} dt = \hat{\varphi}(2\pi k).
 \end{aligned}$$

Hence by using the previous results we have

$$\sum_n \varphi(t-n) = c_0 = 1.$$

□

## 2.2.2 Decomposition algorithm

The properties of the scaling function together with the dilation equation enables us to construct a simple algorithm that relates the coefficients of a given function at different scales.

To this end, let  $f \in L^2(\mathbb{R})$ , such that its coefficients are given by

$$s_k^j = \int_{\mathbb{R}} f(t) \varphi_{j,k}(t) dt, \text{ and } d_k^j = \int_{\mathbb{R}} f(t) \psi_{j,k}(t) dt. \quad (2.35)$$

Using (2.5) and (2.4) we get

$$\begin{aligned}
 s_k^j &= \int_{\mathbb{R}} f(t) \sum_l h_l 2^{-(j-1)/2} \varphi(2^{-(j-1)}t - (2k+l)) dt, \\
 &= \sum_l h_l \int_{\mathbb{R}} f(t) 2^{-(j-1)/2} \varphi(2^{-(j-1)}t - (2k+l)) dt, \\
 &= \sum_l h_l s_{2k+l}^{j-1}.
 \end{aligned}$$

Thus we obtain

$$s_k^j = \sum_l h_l s_{2k+l}^{j-1}. \quad (2.36)$$

Similarly, using relation (2.8) we have

$$\begin{aligned}
 d_k^j &= \int_{\mathbb{R}} f(t) \sum_l g_l 2^{-(j-1)/2} \varphi(2^{-(j-1)}t - (2k+l)) dt, \\
 &= \sum_l g_l \int_{\mathbb{R}} f(t) 2^{-(j-1)/2} \varphi(2^{-(j-1)}t - (2k+l)) dt, \\
 &= \sum_l g_l s_{2k+l}^{j-1}.
 \end{aligned}$$

Hence

$$d_k^j = \sum_l g_l s_{2k+l}^{j-1}. \quad (2.37)$$

The figure below represents graphically the procedure for the wavelet decomposition algorithm.

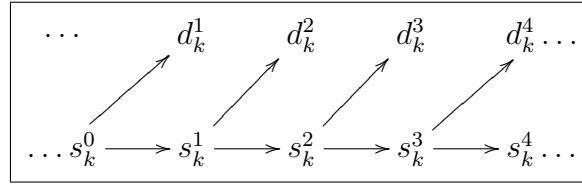


Figure 2.5: The wavelet decomposition algorithm.

The components of the projection of  $f \in V_0$  onto  $V_1$  is given by  $s_k^1$  (2.13) and the error is given by the components  $d_k^1$  of the projection of  $f$  on  $W_1$  (2.14).

### 2.2.3 Reconstruction algorithm

$f \in L^2(\mathbb{R})$ , and let  $P_j f = f_j = \sum_k s_k^j \varphi_{j,k}$  be its projection on  $V_j$ . Referring to (2.12), there exists functions  $f_{j+1} \in V_{j+1}$  and  $g_{j+1} \in W_{j+1}$  such that

$$f_j = f_{j+1} + g_{j+1}.$$

Using the dilation equation (2.5) and the wavelet equation (2.8), we have

$$\begin{aligned}
 \sum_k s_k^j \varphi_{j,k} &= \sum_k s_k^{j+1} \varphi_{j+1,k} + \sum_k d_k^{j+1} \psi_{j+1,k}, \\
 &= \sum_k s_k^{j+1} \sum_l h_l \varphi_{j,2k+l} + \sum_k d_k^{j+1} \sum_l g_l \varphi_{j,2k+l}, \\
 &= \sum_k s_k^{j+1} \sum_l h_{l-2k} \varphi_{j,l} + \sum_k d_k^{j+1} \sum_l g_{l-2k} \varphi_{j,l},
 \end{aligned}$$

$$= \sum_l \left( \sum_k s_k^{j+1} h_{l-2k} + \sum_k d_k^{j+1} g_{l-2k} \right) \varphi_{j,l},$$

where we obtain

$$s_l^j = \sum_k s_k^{j+1} h_{l-2k} + \sum_k d_k^{j+1} g_{l-2k}$$

which is the reconstruction algorithm.

The figure below represents graphically the procedure for the wavelet reconstruction algorithm.

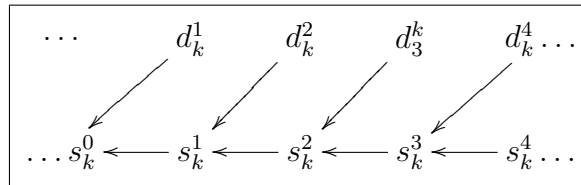


Figure 2.6: The wavelet reconstruction algorithm.

For example, Figure 2.6 illustrates the reconstruction of the coefficients  $s_k^0$  from  $s_k^1$  and  $d_k^1$ .

**Definition 2.2.** Let  $n \in \mathbb{Z}$  and  $n \leq \alpha < n + 1$ . A function is said to be uniformly Lipschitz if there exists a constant  $K$  such that for all  $x, y \in \mathbb{R}$  we have

$$|f^n(x) - f^n(y)| \leq K|x - y|^{\alpha-n}$$

**Theorem 2.1.** Let  $0 < \alpha < n$  be a real number that is not an integer. Let  $f(t) \in L^2(\mathbb{R})$  and  $[a, b]$  be an interval. The function  $f(t)$  is uniformly Lipschitz of order  $\alpha$  over the interval  $[a, b]$  if and only if for any  $n \in \mathbb{Z}$  such that  $2^{-j}n \in (a, b)$ ,

$$|d_n^j| = |\langle f, \psi_{j,n} \rangle| = O(2^{(-\alpha+1/2)j}).$$

The proof of this Theorem can be found in Meyer’s book [24].

This result shows that the decay of the wavelet coefficients depends on the local smoothness of the function in a window determined by the choice of the resolution  $j$ . The larger the constant  $\alpha$ , the faster the decay of the wavelet coefficients. By examining the coefficient of a function’s wavelet transform, we then have a powerful method to investigate a function’s local behaviour. Figure 2.7 demonstrates such localized predominance of wavelet coefficients near the singularities. Therefore this automatic localisation is extremely useful in solving differential equations.

**Example 2.4.** (Decomposition algorithm) Let us consider the function  $f$  defined by

$$f(t) = \begin{cases} \frac{1}{2}t^2 & t \in [0, 1), \\ \frac{1}{2}(-2t^2 + 6t - 3) & t \in [1, 2), \\ \frac{1}{2}(3 - t)^2 & t \in [2, 3), \\ 0 & t \in \mathbb{R} - [0, 3), \end{cases}$$

and the *Lagrange projector* defined by

$$L_j f := \sum_k 2^{j/2} f(2^j k) \varphi_{j,k} \quad (2.38)$$

to approximate the function at any level- $j$ .

The function  $f$  is finitely supported, and possesses discontinuities in the second derivative at  $x \in \{0, 1, 2, 3\}$ .

We use (2.38) to project the function  $f$  at level  $N = -10$  of resolution where the coefficients are given by

$$S_k^N = 2^{N/2} f(2^N k).$$

Together with the decomposition algorithm (2.36), (2.37) based on the Daubechies wavelet of order 4, we show how wavelets detect efficiently the singularities in the second derivatives  $f''$  at  $t \in \{0, 1, 2, 3\}$ .

Observe from Figure 2.7 that the discontinuity in the second derivative  $f''$  is not visible to the human eye. However, the wavelets "see" it according to Theorem 2.1.

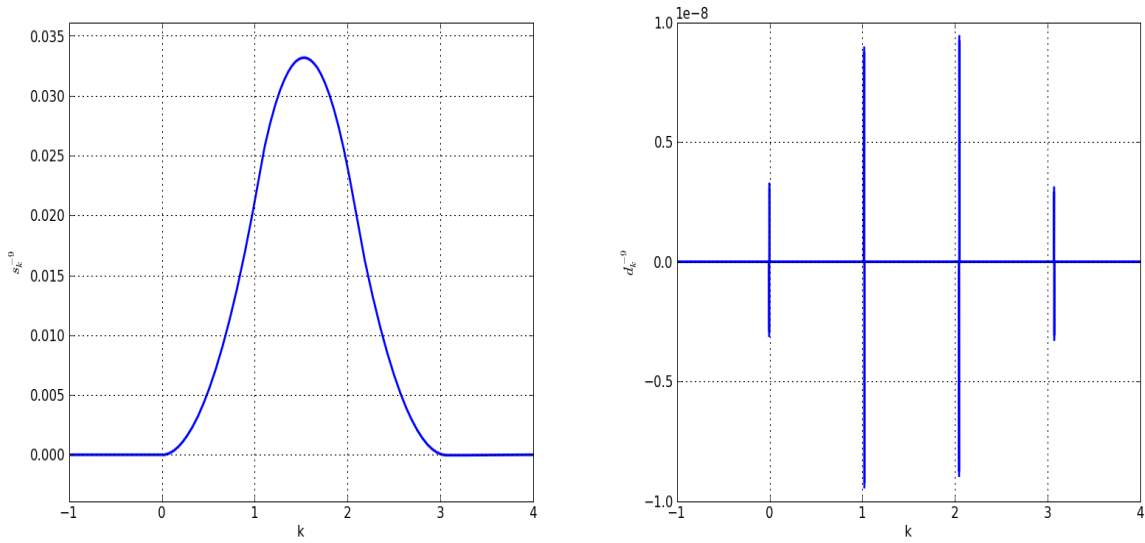


Figure 2.7: The coefficients  $\{s_k^j : k \in \mathbb{Z}\}$  and  $\{d_k^j : k \in \mathbb{Z}\}$  at level  $j = -9$

## 2.3 Wavelets in two dimensions

To obtain an orthogonal basis of  $L^2(\mathbb{R}^2)$  from an orthogonal basis  $(e_i)_{i \in I}$  of  $L^2(\mathbb{R})$ , one can use the tensorial approach which is defined by

$$e_i \otimes e_j(x, y) = e_i(x)e_j(y),$$

where  $\otimes$  denotes the tensor product. Thus  $(e_i \otimes e_j)_{(i,j) \in I^2}$  is an orthogonal basis of  $L^2(\mathbb{R}^2)$ .

Since  $W_j$  is the orthogonal complement of  $V_j$  in  $V_{j-1}$ , we have

$$\begin{aligned} V_{j-1} \otimes V_{j-1} &= (V_j \oplus W_j) \otimes (V_j \oplus W_j), \\ &= (V_j \otimes V_j) \oplus (V_j \otimes W_j) \oplus (W_j \otimes V_j) \oplus (W_j \otimes W_j), \end{aligned}$$

and we repeat with  $V_j \otimes V_j$ . Hence we obtain a decomposition of  $L^2(\mathbb{R}^2)$  given by

$$L^2(\mathbb{R}^2) = \bigoplus_{j \in \mathbb{Z}} ((V_j \otimes W_j) \oplus (W_j \otimes V_j) \oplus (W_j \otimes W_j)),$$

with the basis functions of  $V_j \otimes W_j$ ,  $W_j \otimes V_j$ , and  $W_j \otimes W_j$  given respectively by

$$\begin{cases} \psi^1(x, y) = \varphi(x)\psi(y), \\ \psi^2(x, y) = \psi(x)\varphi(y), \\ \psi^3(x, y) = \psi(x)\psi(y). \end{cases} \quad (2.39)$$

## 2.4 Biorthogonal wavelets

The biorthogonal wavelets are the dual Riesz basis of wavelets defined by

$$\begin{aligned} \tilde{\varphi}(t) &= \sqrt{2} \sum_k \tilde{h}_k \tilde{\varphi}(2t - k), \\ \tilde{\psi}(t) &= \sqrt{2} \sum_k \tilde{g}_k \tilde{\varphi}(2t - k). \end{aligned}$$

They form a multiresolution analysis, that is

$$\cdots, \tilde{V}_2 \subset \tilde{V}_1 \subset \tilde{V}_0 \subset \tilde{V}_{-1} \subset \tilde{V}_{-2} \cdots \subset L^2(\mathbb{R}),$$

with

$$\tilde{V}_{j-1} = \tilde{V}_j \oplus \tilde{W}_j.$$

They also satisfy the following relations

$$\begin{aligned} \int_{\mathbb{R}} \varphi(t) \tilde{\varphi}(t - k) &= \delta_{k,0}, \\ \int_{\mathbb{R}} \varphi(t) \tilde{\psi}(t - k) &= 0, \\ \int_{\mathbb{R}} \psi(t) \tilde{\varphi}(t - k) &= 0, \\ \int_{\mathbb{R}} \psi(t) \tilde{\psi}(t - k) &= \delta_{k,0}. \end{aligned}$$

The projections of a function  $f$  onto the subspace  $V_j$  and the subspace  $W_j$  are given by

$$\begin{aligned} P_j f(t) &= \sum_k \langle f(t), \tilde{\varphi}_{j,k} \rangle \varphi_{j,k}(t), \\ Q_j f(t) &= \sum_k \langle f(t), \tilde{\psi}_{j,k} \rangle \psi_{j,k}(t). \end{aligned}$$



**Remark 2.4.** In the case of orthogonal wavelets we have  $\tilde{h}_k = h_k$ , and  $\tilde{g}_k = g_k$ .

Hence

$$\begin{aligned}\tilde{\varphi}(t) &= \varphi(t) \Rightarrow \tilde{V}_j = V_j, \\ \tilde{\psi}(t) &= \psi(t) \Rightarrow \tilde{W}_j = W_j.\end{aligned}$$

## 2.5 Multiresolution on the interval

When the analyzed function is defined on an interval on the finite interval or if it is periodic, special techniques are developed to handle such a case.

One of these techniques is to periodize the basis function by adding the left-overs from one boundary to the other side [12].

This is done by picking a basis function  $\varphi_{j,k}$  whose support intersects the unit interval and adding to it, its integer translates. Formally, we construct the sum

$$\tilde{\varphi}_{j,k}(t) = \sum_p \varphi_{j,k}(t+p) = 2^{-j/2} \sum_p \varphi(2^{-j}t + 2^{-j}p - k), \quad j \leq 0, \quad k \in \mathbb{Z}, \quad (2.40)$$

and restrict it to  $[0, 1]$ . If  $\varphi_{j,k}$  is fully supported in the unit interval, then it is the only term that contributes to  $\tilde{\varphi}_{j,k}$ . If the  $\text{supp}(\varphi_{j,k})$  contains 0 but not 1, then

$$\tilde{\varphi}_{j,k} = \varphi_{j,k} + \varphi_{j,k+p}$$

and in the opposite situation

$$\tilde{\varphi}_{j,k} = \varphi_{j,k} + \varphi_{j,k-p}.$$

For  $j = 0$ , only one basis function is generated since

$$\tilde{\varphi}_{0,k}(t) = \sum_p \varphi(t+p-k) = 1. \quad (2.41)$$

Note that the 1-periodicity of  $\tilde{\varphi}_{j,k}$  can be verified as

$$\tilde{\varphi}_{j,k}(t+1) = \tilde{\varphi}_{j,k}(t).$$

By doing so, we then obtain a MRA  $\tilde{V}_j$  as the span of all  $\tilde{\varphi}_{j,k}$ , and the wavelet space  $\tilde{W}_j$  spanned by  $\tilde{\psi}_{j,k}$  which are obtained from  $\psi_{j,k}$  in the same manner as  $\tilde{\varphi}_{j,k}$ .

---

The above procedure preserves all the nice properties of the wavelet over the real line that is the orthogonality of the basis function and the vanishing moment property.

These periodic wavelets are useful when dealing with problems with periodic boundary conditions, or with two-point boundary value problems.

# 3. Representation of operators in wavelet basis

In this chapter we consider the representation of operators in the bases of compactly supported wavelets, as discussed in [14]. We begin with the *standard form* (S-form) in Section 3.1, and proceed to the *Non-standard form* (NS-form) in Section 3.2. In Section 3.3, we construct the NS-form of the differential operator, followed by the NS-form of operator functions of  $\partial_x$ . Finally, we give some examples of representation of well-known operators.

## 3.1 The standard form

We are concerned with the representation of Calderón-Zygmund and pseudo-differential operators defined below

**Definition 3.1.** A bounded integral operator  $L$  defined [17] by

$$(Lf)(x) = \int K(x, y)f(y)dy \tag{3.1}$$

is called Calderón-Zygmund if the kernel satisfies

$$\begin{aligned} |K(x, y)| &\leq \frac{C}{|x - y|} \\ \left| \frac{\partial^M}{\partial x^M} K(x, y) + \frac{\partial^M}{\partial y^M} K(x, y) \right| &\leq \frac{C}{|x - y|^{M+1}} \end{aligned}$$

for some  $M \in \mathbb{N}$ .

A pseudo-differential operator  $L$  is a generalization of a differential operator and is defined by a formula of the form

$$(Lf)(x) = \frac{1}{2\pi} \int e^{ix\xi} \sigma(x, \xi) \hat{f}(\xi) d\xi,$$

where  $\sigma(x, \xi)$  the *symbol* of  $L$ , is a polynomial in  $\xi$  whose coefficients are functions in  $x$ .

A pseudo-differential operator is in fact a Calderón-Zygmund operator under certain boundedness

conditions on the symbol  $\sigma(x, \xi)$ , as given in [20].

The standard form is obtained by expanding the operator  $L$  in a telescopic series that is

$$L = \sum_j \left( Q_j L Q_j + \sum_{j' \geq j+1} (Q_{j'} L Q_j + Q_j L Q_{j'}) \right). \quad (3.2)$$

To get the components of the expansion (6.2), we proceed by projecting the kernel  $K(x, y)$  onto a basis generated by the tensor product of wavelets (Subsection 2.3)

$$K(x, y) = \sum_{j,k} \sum_{j',k'} \alpha_{k,k'}^{j,j'} \psi_{j,k}(x) \psi_{j',k'}(y), \quad (3.3)$$

where

$$\alpha_{k,k'}^{j,j'} = \langle K(x, y), \psi_{j,k}(x) \psi_{j',k'}(y) \rangle = \int_{\mathbb{R}} \int_{\mathbb{R}} \psi_{j,k}(x) K(x, y) \psi_{j',k'}(y) dx dy.$$

Using (2.10), any function  $f \in L^2(\mathbb{R})$  may be written as

$$f(y) = \sum_{m,l} f_{m,l} \psi_{m,l}(y). \quad (3.4)$$

Therefore, substituting (3.3) and (3.4) in (3.1), and assuming that the interchanges of summation and integration are justified ([10],[14]), we have

$$\begin{aligned} Lf(x) &= \int_{\mathbb{R}} \sum_{j,k} \sum_{j',k'} \alpha_{k,k'}^{j,j'} \psi_{j,k}(x) \psi_{j',k'}(y) \sum_{m,l} f_{m,l} \psi_{m,l}(y) dy, \\ &= \sum_{m,l} \sum_{j,k} \sum_{j',k'} \alpha_{k,k'}^{j,j'} f_{m,l} \psi_{j,k}(x) \int_{\mathbb{R}} \psi_{j',k'}(y) \psi_{m,l}(y) dy, \\ &= \sum_{m,l} \sum_{j,k} \sum_{j',k'} \alpha_{k,k'}^{j,j'} f_{m,l} \psi_{j,k}(x) \delta_{j'k',ml}, \\ &= \sum_{j,k} \sum_{j',k'} \alpha_{k,k'}^{j,j'} f_{j',k'} \psi_{j,k}(x), \end{aligned}$$

where

$$\delta_{ik,jl} = \begin{cases} 1 & \text{if } i = j \text{ and } k = l, \\ 0 & \text{otherwise.} \end{cases}$$

On the other hand, the projection of  $f$  onto subspaces  $W_p$  is given by  $Q_p f(y) = \sum_l f_{p,l} \psi_{p,l}(y)$ .

Thus

$$L(Q_p f)(x) = \int_{\mathbb{R}} \sum_{j,k} \sum_{j',k'} \alpha_{k,k'}^{j,j'} \psi_{j,k}(x) \psi_{j',k'}(y) \sum_l f_{p,l} \psi_{p,l}(y) dy,$$

$$\begin{aligned}
&= \sum_l \sum_{j,k} \sum_{j',k'} \alpha_{k,k'}^{j,j'} f_{p,l} \psi_{j,k}(x) \int_{\mathbb{R}} \psi_{j',k'}(y) \psi_{p,l}(y) dy, \\
&= \sum_l \sum_{j,k} \sum_{j',k'} \alpha_{k,k'}^{j,j'} f_{p,l} \psi_{j,k}(x) \delta_{j'k',pl}, \\
&= \sum_{j,k} \sum_{k'} \alpha_{k,k'}^{j,p} f_{p,k'} \psi_{j,k}(x). \tag{3.5}
\end{aligned}$$

Projecting the result (3.5) onto  $W_p$  again gives [10]

$$Q_p(\mathbf{L}Q_p f)(x) = \sum_n \langle \mathbf{L}(Q_p f)(y), \psi_{p,n}(y) \rangle \psi_{p,n}(x), \tag{3.6}$$

$$= \sum_n \int_{\mathbb{R}} \left( \sum_{j,k} \sum_{k'} \alpha_{k,k'}^{j,p} f_{p,k'} \psi_{j,k}(y) \right) \psi_{p,n}(y) dy \psi_{p,n}(x), \tag{3.7}$$

$$= \sum_n \sum_{j,k} \sum_{k'} \alpha_{k,k'}^{j,p} f_{p,k'} \psi_{p,n}(x) \int_{\mathbb{R}} \psi_{j,k}(y) \psi_{p,n}(y) dy, \tag{3.8}$$

$$= \sum_n \sum_{k'} \alpha_{n,k'}^{p,p} f_{p,k'} \psi_{p,n}(x). \tag{3.9}$$

Hence

$$Q_j(\mathbf{L}Q_j f)(x) = \sum_k \left( \sum_{k'} \alpha_{k,k'}^j f_{j,k'} \right) \psi_{j,k}(x),$$

with

$$\alpha_{k,k'}^j := \alpha_{k,k'}^{jj} = \int_{\mathbb{R}} \int_{\mathbb{R}} \psi_{j,k}(x) K(x,y) \psi_{j,k'}(y) dx dy. \tag{3.10}$$

Similarly, we find

$$Q_j(\mathbf{L}Q_{j'} f)(x) = \sum_k \left( \sum_{k'} \beta_{k,k'}^{j,j'} f_{j',k'} \right) \psi_{j,k}(x),$$

$$Q_{j'}(\mathbf{L}Q_j f)(x) = \sum_k \left( \sum_{k'} \gamma_{k,k'}^{j',j} f_{j,k'} \right) \psi_{j',k}(x),$$

where

$$\beta_{k,k'}^{j,j'} = \int_{\mathbb{R}} \int_{\mathbb{R}} \psi_{j,k}(x) K(x,y) \psi_{j',k'}(y) dx dy, \tag{3.11}$$

and

$$\gamma_{k,k'}^{j',j} = \int_{\mathbb{R}} \int_{\mathbb{R}} \psi_{j',k}(x) K(x,y) \psi_{j,k'}(y) dx dy. \tag{3.12}$$

Let the operators  $A_j$ ,  $B_j^{j'}$ , and  $\Gamma_j^{j'}$  be defined by

$$A_j = Q_j \mathbf{L} Q_j : W_j \rightarrow W_j, \tag{3.13}$$

$$B_j^{j'} = Q_j L Q_{j'} : W_{j'} \rightarrow W_j, \quad (3.14)$$

$$\Gamma_j^{j'} = Q_{j'} L Q_j : W_j \rightarrow W_{j'}, \quad (3.15)$$

and be represented respectively by the matrices  $\alpha^j, \beta^{j,j'}$ , and  $\gamma^{j,j'}$  for  $j = 1, 2, \dots, n$  and  $j' = j + 1, \dots, n$ .

The standard form (S-form) is the representation of an operator L in the wavelet bases by the set of operators

$$L = \{A_j, \{B_j^{j'}\}_{j' \geq j+1}, \{\Gamma_j^{j'}\}_{j' \geq j+1}\}_{j \in \mathbb{Z}}. \quad (3.16)$$

If there is a coarsest scale  $j = n$  and a finest scale  $j = 0$ , then instead of (3.16) we have

$$L \approx L_0 = \{A_j, \{B_j^{j'}\}_{j'=j+1}^{j'=n}, \{\Gamma_j^{j'}\}_{j'=j+1}^{j'=n}, B_j^{n+1}, \Gamma_j^{n+1}, L_n\}_{j=1, \dots, n}, \quad (3.17)$$

with  $L_0 = P_0 L P_0$ , and  $L_n = P_n L P_n$  is represented by the matrix  $s^n$  with entries defined by

$$s_{k,k'}^n = \int_{\mathbb{R}} \int_{\mathbb{R}} \varphi_{n,k}(x) K(x, y) \varphi_{n,k'}(y) dx dy. \quad (3.18)$$

The standard form can be obtained by applying the one-dimensional discrete wavelet transform (2.36) and (2.37) to each column (row) of the discrete version of the operator L in the ordinary domain and then to each row (column) of the result (see Figure 3.1).

Note that the S-form has several 'finger' bands which correspond to the interaction between different scales (see Figure 3.5 Page 42).

$A_1$	$B_1^2$	$B_1^3$	$B_1^4$
$\Gamma_1^2$	$A_2$	$B_2^3$	$B_2^4$
$\Gamma_1^3$	$\Gamma_2^3$	$A_3$	$B_3^4$
$\Gamma_1^4$	$\Gamma_2^4$	$\Gamma_3^4$	$L_3$

Figure 3.1: Organization of a matrix in the standard form.

### 3.2 The Non-standard form

The Non-standard form (NS-form) is a tool developed by Beylkin, Coifman and Rokhlin [14] which aims at preserving as much structure as possible by 'almost' doing a full wavelet decomposition of an operator.

Let  $L$  be an operator

$$L : L^2(\mathbb{R}) \rightarrow L^2(\mathbb{R})$$

and  $L_j = P_j L P_j$  denote its projection onto  $V_j$ .

The NS-form is a representation of the operator  $L$  as a chain of triplets

$$L = \{A_j, B_j, C_j\}_{j \in \mathbb{Z}} \tag{3.19}$$

acting on the subspaces  $V_j$  and  $W_j$ , where  $A_j = Q_j L Q_j$ ,  $B_j = Q_j L P_j$  and  $C_j = P_j L Q_j$  are obtained by expanding  $L$  in a telescopic series, that is,

$$\begin{aligned} L &= \sum_{j \in \mathbb{Z}} P_{j-1} L P_{j-1} - P_j L P_j, \\ &= \sum_{j \in \mathbb{Z}} (P_{j-1} - P_j) L (P_{j-1} - P_j) + (P_{j-1} - P_j) L P_j + P_j L (P_{j-1} - P_j). \end{aligned}$$

Since  $P_{j-1} - P_j = Q_j$  we have

$$\begin{aligned} \mathbf{L} &= \sum_{j \in \mathbb{Z}} Q_j \mathbf{L} Q_j + Q_j \mathbf{L} P_j + P_j \mathbf{L} Q_j, \\ &= \sum_{j \in \mathbb{Z}} A_j + B_j + C_j, \end{aligned}$$

with

$$A_j = Q_j \mathbf{L} Q_j : W_j \rightarrow W_j, \quad (3.20)$$

$$B_j = Q_j \mathbf{L} P_j : V_j \rightarrow W_j, \quad (3.21)$$

$$C_j = P_j \mathbf{L} Q_j : W_j \rightarrow V_j. \quad (3.22)$$

For numerical purposes, we define a finest scale  $j = 0$ , and a coarsest scale  $j = n$ , such that we have

$$\mathbf{L} \approx \mathbf{L}_0 = \{ \{ A_j, B_j, C_j \}_{j=1,2,\dots,n}, \mathbf{L}_n \} \quad (3.23)$$

with  $\mathbf{L}_0 = P_0 \mathbf{L} P_0$ , and  $\mathbf{L}_n = P_n \mathbf{L} P_n$ .

Another way to understand the NS-form is an analogy with the two-dimensional MRA, where the wavelet basis is given in (2.3). Therefore, the decomposition of an operator in this wavelet basis yields the NS-form (see Figure 3.2).

In fact, the decomposition of  $\mathbf{L}_j$  in  $W_j$  is  $A_j + B_j + C_j$  while the projection onto  $V_j$ .

The operators  $A_j$ ,  $B_j$ ,  $C_j$  and  $\mathbf{L}_j$  are represented respectively by the matrices  $\alpha^j$ ,  $\beta^j$ ,  $\gamma^j$  and  $s^j$ , with entries given by

$$\begin{aligned} \alpha_{k,k'}^j &= \int_{\mathbb{R}} \int_{\mathbb{R}} \psi_{j,k}(x) K(x,y) \psi_{j,k'}(y) dx dy, \\ \beta_{k,k'}^j &= \int_{\mathbb{R}} \int_{\mathbb{R}} \psi_{j,k}(x) K(x,y) \varphi_{j,k'}(y) dx dy, \\ \gamma_{k,k'}^j &= \int_{\mathbb{R}} \int_{\mathbb{R}} \varphi_{j,k}(x) K(x,y) \psi_{j,k'}(y) dx dy, \\ s_{k,k'}^j &= \int_{\mathbb{R}} \int_{\mathbb{R}} \varphi_{j,k}(x) K(x,y) \varphi_{j,k'}(y) dx dy. \end{aligned} \quad (3.24)$$



Using (2.5) in (3.24), we have

$$\begin{aligned}
 s_{k,k'}^j &= \int_{\mathbb{R}} \int_{\mathbb{R}} \sum_{l=0}^{L-1} h_l \varphi_{j-1,2k+l}(x) K(x, y) \sum_{l'=0}^{L-1} h_{l'} \varphi_{j-1,2k'+l'}(y) dx dy, \\
 &= \sum_{l=0}^{L-1} \sum_{l'=0}^{L-1} h_l h_{l'} \int_{\mathbb{R}} \int_{\mathbb{R}} \varphi_{j-1,2k+l}(x) K(x, y) \varphi_{j-1,2k'+l'}(y) dx dy, \\
 &= \sum_{l=0}^{L-1} \sum_{l'=0}^{L-1} h_l h_{l'} s_{2k+l,2k'+l'}^{j-1}.
 \end{aligned}$$

Similarly, we obtain

$$\begin{aligned}
 \alpha_{k,k'}^j &= \sum_{l=0}^{L-1} \sum_{l'=0}^{L-1} g_l g_{l'} s_{2k+l,2k'+l'}^{j-1}, \\
 \beta_{k,k'}^j &= \sum_{l=0}^{L-1} \sum_{l'=0}^{L-1} g_l h_{l'} s_{2k+l,2k'+l'}^{j-1}, \\
 \gamma_{k,k'}^j &= \sum_{l=0}^{L-1} \sum_{l'=0}^{L-1} h_l g_{l'} s_{2k+l,2k'+l'}^{j-1}.
 \end{aligned}$$

A <sub>1</sub>	B <sub>1</sub>				
C <sub>1</sub>					
		A <sub>2</sub>	B <sub>2</sub>		
		C <sub>2</sub>			
				A <sub>3</sub>	B <sub>3</sub>
				C <sub>3</sub>	L <sub>3</sub>

Figure 3.2: Organization of the non-standard form of a matrix. Blanks denote zero entries.

### 3.3 Non-Standard form representation of the operator $\frac{d^p}{dx^p}$

Let us consider a differential operator of the form  $L = \frac{d^p}{dx^p}$ . The process of determining the representation is slightly different, but the end result is as mentioned previously, where  $\frac{d^p}{dx^p} \varphi_{j,k}(x) = \varphi_{j,k}^{(p)}(x)$ .

For  $P_j f(x) = \sum_k s_k^j \varphi_{j,k}$ , we have

$$LP_j f(x) = \frac{d^p}{dx^p} P_j f(x) = \sum_{k'} s_{k'}^j \varphi_{j,k'}^{(p)}(x).$$

But  $\frac{d^p}{dx^p} \varphi_{j,k'}(x)$  might not be in  $V_j$ , so we project again

$$\begin{aligned} P_j LP_j f(x) &= \sum_k \left\langle \sum_{k'} s_{k'}^j \varphi_{j,k'}^{(p)}(x), \varphi_{j,k}(x) \right\rangle \varphi_{j,k}, \\ &= \sum_k \left( \sum_{k'} s_{k'}^j r_{k,k'}^j \right) \varphi_{j,k}, \end{aligned}$$

where

$$r_{k,k'}^j = \int_{\mathbb{R}} \varphi_{j,k}(x) \varphi_{j,k'}^{(p)}(x) dx. \quad (3.25)$$

Similarly, we have

$$\begin{aligned} \alpha_{k,k'}^j &= \int_{\mathbb{R}} \psi_{j,k}(x) \psi_{j,k'}^{(p)}(x) dx, \\ \beta_{k,k'}^j &= \int_{\mathbb{R}} \psi_{j,k}(x) \varphi_{j,k'}^{(p)}(x) dx, \\ \gamma_{k,k'}^j &= \int_{\mathbb{R}} \varphi_{j,k}(x) \psi_{j,k'}^{(p)}(x) dx. \end{aligned}$$

The  $r_{k,k'}^j$  may be simplified as

$$\begin{aligned} r_{k,k'}^j &= \int_{\mathbb{R}} 2^{-\frac{j}{2}} \varphi(2^{-j}x - k) \frac{d^p}{dx^p} \left( 2^{-\frac{j}{2}} \varphi(2^{-j}x - k') \right) dx, \\ &= 2^{-jp} \int_{\mathbb{R}} \varphi(x' - (k - k')) \varphi^{(p)}(x') dx', \quad (x' = 2^{-j}x - k'), \\ &= 2^{-jp} r_{k-k',0}^0, \\ &= 2^{-jp} r_l^0, \quad (l = k - k', \text{ and } r_l^0 := r_{l,0}^0) \end{aligned}$$

where

$$r_l^0 = \int_{\mathbb{R}} \varphi(x - l) \varphi^{(p)}(x) dx. \quad (3.26)$$

Similarly, with  $l = k - k'$

$$\begin{aligned}\alpha_{k,k'}^j &= 2^{-jp} \alpha_l^0, \\ \beta_{k,k'}^j &= 2^{-jp} \beta_l^0, \\ \gamma_{k,k'}^j &= 2^{-jp} \gamma_l^0,\end{aligned}$$

where

$$\begin{aligned}\alpha_l^0 &= \int_{\mathbb{R}} \psi(x-l) \psi^{(p)}(x) dx, \\ \beta_l^0 &= \int_{\mathbb{R}} \psi(x-l) \varphi^{(p)}(x) dx, \\ \gamma_l^0 &= \int_{\mathbb{R}} \varphi(x-l) \psi^{(p)}(x) dx.\end{aligned}$$

Using (2.5) in (3.26), we have

$$\begin{aligned}r_l^0 &= \int_{\mathbb{R}} \left( \sqrt{2} \sum_{k=0}^{L-1} h_k \varphi(2x - 2l - k) \right) \frac{d^p}{dx^p} \left( \sqrt{2} \sum_{k'=0}^{L-1} h_{k'} \varphi(2x - k') \right) dx, \\ &= 2^p \sum_{k=0}^{L-1} \sum_{k'=0}^{L-1} h_k h_{k'} \int_{\mathbb{R}} \varphi(x' - (2l + k - k')) \varphi^{(p)}(x') dx', \quad (x' = 2x - k') \\ &= 2^p \sum_{k=0}^{L-1} \sum_{k'=0}^{L-1} h_k h_{k'} r_{2l+k-k'}^0.\end{aligned}\tag{3.27}$$

Similarly for  $\alpha_l^0, \beta_l^0$  and  $\gamma_l^0$

$$\begin{aligned}\alpha_l^0 &= 2^p \sum_{k=0}^{L-1} \sum_{k'=0}^{L-1} g_k g_{k'} r_{2l+k-k'}^0, \\ \beta_l^0 &= 2^p \sum_{k=0}^{L-1} \sum_{k'=0}^{L-1} g_k h_{k'} r_{2l+k-k'}^0, \\ \gamma_l^0 &= 2^p \sum_{k=0}^{L-1} \sum_{k'=0}^{L-1} h_k g_{k'} r_{2l+k-k'}^0.\end{aligned}$$

Using Parseval's relation (2.3)  $r_l^0$  satisfies

$$\begin{aligned}r_l^0 &= \langle \varphi_{0,l}, \varphi^{(p)} \rangle, \\ &= \frac{1}{2\pi} \langle \hat{\varphi}_{0,l}, \hat{\varphi}^{(p)} \rangle, \\ &= (-1)^p r_{-l}^0.\end{aligned}$$

We notice that the NS-form of the operator  $\frac{d^p}{dx^p}$  is completely determined by its coefficients  $r_l^0$  of its projection in the subspace  $V_0$ . Therefore we are led to compute the coefficients  $r_l^0$  which becomes a problem of solving for connection coefficients denoted by

$$\Lambda_l^{d_1, d_2} = \int \varphi^{(d_1)}(x-l)\varphi^{(d_2)}(x)dx.$$

**Remark 3.1.** If  $d_1 = 0$  and  $d_2 = p$ , we have  $\Lambda_l^{0,p} \equiv r_l^0$ .

Substituting  $n = k - k'$  in (3.27) we get

$$\begin{aligned} r_l^0 &= 2^p \sum_{k=0}^{L-1} \sum_{n=k-L+1}^k h_k h_{k-n} r_{2l+n}^0, \\ &= 2^p \sum_{n=-L+1}^{-1} \sum_{k=0}^{n+L-1} h_k h_{k-n} r_{2l+n}^0 + 2^p \sum_{k=0}^{L-1} h_k^2 r_{2l}^0 + 2^p \sum_{n=1}^{L-1} \sum_{k=n}^{L-1} h_k h_{k-n} r_{2l+n}^0, \\ &= 2^p \sum_{n=-L+1}^{-1} r_{2l+n}^0 \sum_{k=0}^{n+L-1} h_k h_{k-n} + 2^p r_{2l}^0 \sum_{k=0}^{L-1} h_k^2 + 2^p \sum_{n=1}^{L-1} r_{2l+n}^0 \sum_{k=n}^{L-1} h_k h_{k-n}. \end{aligned} \quad (3.28)$$

Additionally we have the autocorrelation coefficients defined by

$$a_m = 2 \sum_{i=0}^{L-1-m} h_i h_{i+m}, \quad m = 1, \dots, L-1.$$

For  $m = 2k$ , it can be shown that ([4],[5])  $a_{2k} = 0$ ,  $k = 1, \dots, L/2 - 1$ .

So, for  $2 - L \leq l \leq L - 2$  and using (2.25)  $\sum_{k=0}^{L-1} h_k^2 = 1$ , equation (3.28) becomes

$$\begin{aligned} r_l^0 &= 2^p \sum_{n=-L+1}^{-1} r_{2l+n}^0 \frac{1}{2} a_{-n} + 2^p r_{2l}^0 \sum_{k=0}^{L-1} h_k^2 + 2^p \sum_{n=1}^{L-1} r_{2l+n}^0 \frac{1}{2} a_n, \\ &= 2^{p-1} \sum_{k=-L/2}^{-1} r_{2l+2k+1}^0 a_{-2k-1} + 2^{p-1} \sum_{k=-(L-2)/2}^{-1} r_{2l+2k}^0 a_{-2k} + 2^p r_{2l}^0 \sum_{k=0}^{L-1} h_k^2 \\ &\quad + 2^{p-1} \sum_{k=1}^{L/2} r_{2l+2k-1}^0 a_{2k-1} + 2^{p-1} \sum_{k=1}^{L-2/2} r_{2l+2k}^0 a_{2k}, \\ &= 2^p r_{2l}^0 + 2^{p-1} \sum_{k=1}^{L/2} a_{2k-1} (r_{2l-2k+1}^0 + r_{2l+2k-1}^0). \end{aligned} \quad (3.29)$$

The result (3.29) does not guarantee a unique solution, therefore we need a normalization condition.

To this end, we use the moment of scaling function defined by

$$\mathcal{M}_l^\varphi = \int_{\mathbb{R}} \varphi(x) x^l dx, \quad l = 1, 2, \dots, m.$$

It can be shown according to [3] that

$$\sum_k k^m \varphi(x - k) = x^m + \sum_{l=1}^m (-1)^l \binom{m}{l} \mathcal{M}_l^\varphi x^{m-l},$$

and a suitable normalization condition is

$$\sum_{l=2-L}^{L-2} l^p r_l^0 = (-1)^p p!. \quad (3.30)$$

**Remark 3.2.** For  $p=1$ , the coefficients  $r_l^0$  are found in [3].

## 3.4 The NS-form of operator functions

In this section, we consider the NS-form of the analytic function of the differential operator  $\partial_x$ , that is,

$$f(\partial_x) = e^{\Delta t \mathcal{L}} \quad (3.31)$$

where  $\mathcal{L} = \partial_x^p$ .

The representation of this operator in the wavelet basis is of prime importance because it appears in the solution of partial differential equations using the semigroup approach.

There are two approaches for computing the NS-forms of operator functions. Both are valid due to the analyticity of the function  $f$ :

(i) compute the projection of the operator function on  $V_0$ ,

$$P_0 f(\partial_x) P_0, \quad (3.32)$$

or,

(ii) compute the function of the projection of the operator,

$$f(P_0 \partial_x P_0). \quad (3.33)$$

First we consider the representation given by (3.32). We must find  $r_{k,k'}^j$  of the form

$$r_{k,k'}^j = \int_{\mathbb{R}} \varphi_{j,k}(x) f(\partial_x) \varphi_{j,k'}(x) dx. \quad (3.34)$$

For  $f$  analytic and  $f, g \in L^2(\mathbb{R})$ , the relation  $\mathcal{F}(f(\partial_x)g(x))(\xi) = f(i\xi)\hat{g}(\xi)$  holds (see [8]).

Hence

$$\begin{aligned} \mathcal{F}(f(\partial_x)(\varphi(2^{-j}x - k')))(\xi) &= f(i\xi) \int_{\mathbb{R}} \varphi(2^{-j}x - k') e^{-ix\xi} dx, \\ &= 2^j f(i\xi) \int_{\mathbb{R}} \varphi(x') e^{-i\xi 2^j(x'+k')} dx', \quad (x' = 2^{-j}x - k), \\ &= 2^j f(i\xi) e^{-i\xi 2^j k'} \int_{\mathbb{R}} \varphi(x') e^{-i\xi 2^j x'} dx', \\ &= 2^j f(i\xi) e^{-i\xi 2^j k'} \hat{\varphi}(\xi 2^j). \end{aligned}$$

Taking the inverse Fourier transform, we have

$$f(\partial_x)(\varphi(2^{-j}x - k')) = \frac{1}{2\pi} \int_{\mathbb{R}} 2^j f(i\xi) e^{-i\xi 2^j k'} \hat{\varphi}(\xi 2^j) e^{ix\xi} d\xi.$$

Therefore (3.34) may be rewritten as

$$\begin{aligned} r_{k,k'}^j &= \frac{1}{2\pi} \int_{\mathbb{R}} \varphi(2^{-j}x - k) \int_{\mathbb{R}} f(i\xi) e^{-i\xi 2^j k'} \hat{\varphi}(\xi 2^j) e^{ix\xi} d\xi dx, \\ &= \frac{2^{-j}}{2\pi} \int_{\mathbb{R}} \varphi(2^{-j}x - k) \int_{\mathbb{R}} f(i2^{-j}\rho) e^{-i\rho k'} \hat{\varphi}(\rho) e^{ix2^{-j}\rho} d\rho dx, \quad (\rho = 2^j\xi), \\ &= \frac{1}{2\pi} \int_{\mathbb{R}} \int_{\mathbb{R}} \varphi(x') \hat{\varphi}(\rho) e^{-i\rho k'} e^{i\rho(x'+k)} dx' f(i2^{-j}\rho) d\rho, \\ &= \frac{1}{2\pi} \int_{\mathbb{R}} \left( \int_{\mathbb{R}} \varphi(x') e^{i\rho x'} dx' \right) \hat{\varphi}(\rho) e^{i\rho(k-k')} f(i2^{-j}\rho) d\rho, \\ &= \frac{1}{2\pi} \int_{\mathbb{R}} \overline{\hat{\varphi}(\rho)} \hat{\varphi}(\rho) e^{i\rho(k-k')} f(i2^{-j}\rho) d\rho. \end{aligned}$$

Setting  $l = k - k'$  we have

$$\begin{aligned} r_l^j &= \frac{1}{2\pi} \int_{\mathbb{R}} f(i2^{-j}\rho) |\hat{\varphi}(\rho)|^2 e^{i\rho l} d\rho, \\ &= \frac{1}{2\pi} \sum_{k \in \mathbb{Z}} \int_{2\pi k}^{2\pi(k+1)} f(i2^{-j}\rho) |\hat{\varphi}(\rho)|^2 e^{i\rho l} d\rho, \\ &= \frac{1}{2\pi} \int_0^{2\pi} \sum_{k \in \mathbb{Z}} f(i2^{-j}(\rho' + 2\pi k)) |\hat{\varphi}(\rho' + 2\pi k)|^2 e^{i(\rho' + 2\pi k)l} d\rho', \quad (\rho' = \rho - 2\pi k) \\ &= \int_0^{2\pi} g(\rho') e^{i l \rho'} d\rho', \end{aligned}$$

where we define  $g(\rho)$  to be

$$g(\rho) = \frac{1}{2\pi} \sum_{k \in \mathbb{Z}} f(i2^{-j}(\rho + 2\pi k)) |\hat{\varphi}(\rho + 2\pi k)|^2. \quad (3.35)$$

Now the Riemann-Lebesgue lemma states that if  $f \in L^1(\mathbb{R})$ , then its Fourier transform tends to zero as  $\xi$  tends to infinity. Using this lemma, we have for every  $\epsilon > 0$  there exists  $K > 0$ , such that  $|\hat{\varphi}(\rho)|^2 < \epsilon$  for  $|\rho| > K$ . Hence we may use  $|\hat{\varphi}(\rho)|^2$  as a cutoff function, to get an approximation  $g_a$  of  $g$

$$g_a(\rho) = \frac{1}{2\pi} \sum_{k=-K}^K f(i2^{-j}(\rho + 2\pi k)) |\hat{\varphi}(\rho + 2\pi k)|^2. \quad (3.36)$$

We then have

$$r_l^j = \frac{1}{N} \sum_{n=0}^{N-1} g_a(\rho_n) e^{il\rho_n}, \quad \text{where } \rho_n = \frac{2\pi n}{N-1}.$$

Here  $N$  is the number of quadrature points used in approximating the integral.

The coefficients  $r_l^j$  are computed by applying the DFT<sup>1</sup> to the sequence  $\{g_a(\rho_n)\}$ . Before proceeding to compute the NS-form of an operator function by (3.33), we recall the discrete Fourier transform for a vector of length  $N$  is defined by

$$\begin{aligned} (\mathfrak{F}f)_n &= \hat{f}_n = \sum_{j=0}^{N-1} f_j e^{-i2\pi nj/N}, \quad n = 0, 1, \dots, N-1, \\ (\mathfrak{F}^{-1}f)_j &= f_j = \frac{1}{N} \sum_{n=0}^{N-1} \hat{f}_n e^{i2\pi nj/N}, \quad j = 0, 1, \dots, N-1, \end{aligned}$$

where the subscript denotes components.

The NS-form of (3.33) is computed by projecting the operator  $\partial_x$  into the finest subspace  $V_0$  of dimension  $2^n$ . That is,  $\partial_x \approx P_0 \partial_x P_0$ , we therefore have  $f(\partial_x) \approx f(P_0 \partial_x P_0)$ .

Let  $M$  be a bi-infinite Toeplitz matrix representing the operator  $P_0 \partial_x P_0$  with entries

$$M_{i,j} = r_{i-j}^0.$$

Using the DFT, we diagonalize  $M$  that is,

$$M = \mathfrak{F} \Lambda \mathfrak{F}^{-1},$$

---

<sup>1</sup>Discrete Fourier Transform

where  $(\mathfrak{F})_{k,j} = e^{-i2\pi kj/N}$ ,  $(\mathfrak{F}^{-1})_{k,j} = \frac{1}{N}e^{i2\pi kj/N}$ , and  $\Lambda$  is the diagonal matrix with entries given by

$$\lambda_k = r_0^0 + \sum_{j=1}^{L-2} (r_j^0 e^{2i\pi kj/(2L-3)} + r_{-j}^0 e^{-2i\pi kj/(2L-3)}), \quad k = 1, \dots, 2L-3, \quad (3.37)$$

corresponding to the eigenvalues of the matrix  $M$ .

For an analytic function  $f$  in a neighborhood of the spectrum of  $M$ , we have

$$f(M) = \mathfrak{F}f(\Lambda)\mathfrak{F}^{-1}. \quad (3.38)$$

We now proceed by computing the RHS<sup>2</sup> of (3.38).

For any vector  $w$  of length  $N = 2L - 3$ , we have (see [10])

$$(\mathfrak{F}f(\Lambda)\mathfrak{F}^{-1}w)_m = \sum_{j=2-L}^{L-2} w_j \frac{1}{N} \sum_{k=2-L}^{L-2} f(\lambda_k) e^{i2\pi k(j-m)/N}, \quad m = 2-L, \dots, L-2. \quad (3.39)$$

Hence the entries of the matrix  $f(M)$  are given by

$$r_l^0 = \frac{1}{N} \sum_{k=2-L}^{L-2} f(\lambda_k) e^{i2\pi kl/N}. \quad (3.40)$$

Thus we have developed two approaches for computing the coefficient  $r_l^0$  of the matrix  $f(M)$  given by (3.33) or (3.32).

## 3.5 Examples of Representation of operators

**Example 3.1.** Consider the operator  $L = \frac{d^2}{dx^2}$ . We represent this operator in the wavelet domain using the NS-form. We use Daubechies wavelet with 6 vanishing moments and set to zero all entries whose absolute values are smaller than  $10^{-8}$  (see Figure 3.3).

---

<sup>2</sup>right hand side



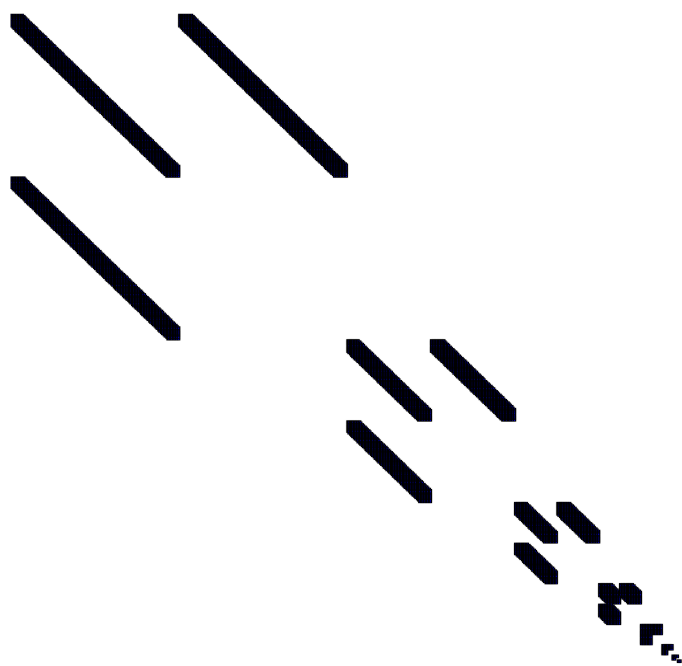


Figure 3.3: The non-standard form of  $\frac{d^2}{dx^2}$ .

**Example 3.2.** Let us consider the Calderón-Zygmund operator defined by its matrix which is smooth with entries decreasing in magnitude away from the diagonal

$$A_{i,j} = \begin{cases} \frac{1}{i-j} & i \neq j, \\ 0 & i = j. \end{cases}$$

By projecting it into wavelet bases in NS-form and S-form with Daubechies wavelet having six vanishing moments, we obtain Figure 3.4 or Figure 3.5 after setting to zero all entries whose absolute values are smaller than  $10^{-7}$ .

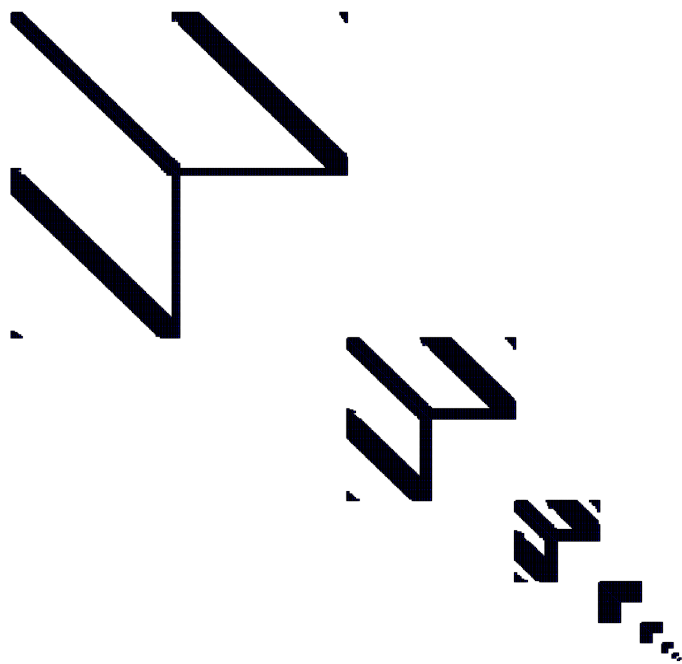


Figure 3.4: The Non-standard form of the Example 3.2

**Example 3.3.** Consider the matrix

$$A_{i,j} = \begin{cases} 1 & |i - j| = 1 \text{ or } N - 1, \\ -2 & i = j, \\ 0 & \text{elsewhere.} \end{cases}$$

We project this operator which corresponds to the periodized version of the second derivative operator into the wavelet domain using the NS-form. We use again Daubechies wavelet with six vanishing moments and setting to zero all entries whose absolute values are smaller than  $10^{-8}$  (see Figure 3.6).

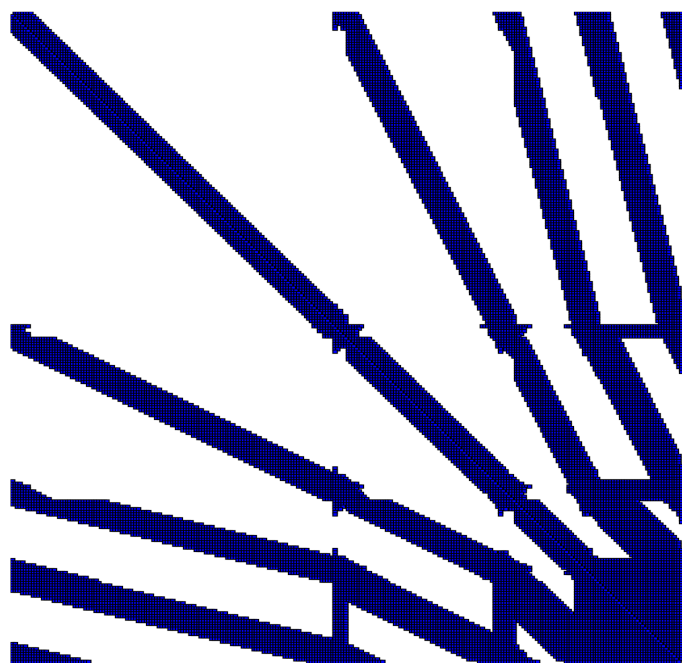


Figure 3.5: The standard form of the Example 3.2



Figure 3.6: The Non-standard form of the Example 3.3

## 4. Wavelets in Linear Algebra

### 4.1 The Inverse Operator in Wavelet Basis

In this Chapter we discuss the implications of wavelets in linear algebra. In fact, a wavelet basis in this case plays the role of a fast solver, since it reduces considerably the condition numbers [2].

To illustrate this, we consider the two-point boundary value problem

$$\begin{cases} \mathcal{L}u(x) = f(x), \\ u(0) = u(1) = 0, \end{cases} \quad (4.1)$$

where

$$\mathcal{L}u = \frac{d}{dx} \left( a(x) \frac{du}{dx} \right) - b(x)u,$$

and  $a(x)$ ,  $b(x)$  are sufficiently smooth functions.

We use the finite difference method to discretize the operator  $\mathcal{L}$  and denote the result by  $\hat{\mathcal{L}}$ , where

$$\hat{\mathcal{L}}u_i = \frac{a_{i+1/2}u_{i+1} - (a_{i+1/2} + a_{i-1/2})u_i + a_{i-1/2}u_{i-1}}{h^2} - b_i u_i. \quad (4.2)$$

Here  $x_i = ih$ ,  $h = \frac{1}{N}$ , and  $a_{i\pm 1/2} = a(x_{i\pm 1/2})$ ,  $u_i = u(x_i)$ ,  $i = 0, 1, \dots, N-1$ , and we have used the central difference approximation with spacing  $h$  to approximate the derivative.

Thus, the problem (4.1) is equivalent to solving a linear system of the form

$$\mathbf{L}\mathbf{u} = \mathbf{f}, \quad (4.3)$$

where  $\mathbf{L}$  is a sparse matrix defined by

$$\mathbf{L} = \text{tridiag} \left( a_{i-1/2}, -(a_{i+1/2} + a_{i-1/2} + h^2 b_i), a_{i+1/2} \right),$$

$\mathbf{u} = (u_0, u_1, \dots, u_{N-1})^T$ ,  $\mathbf{f} = h^2(f_0, f_1, \dots, f_{N-1})^T$ , and  $\text{tridiag}(\cdot, \cdot, \cdot)$  denotes a tridiagonal matrix.

So computing the solution of (4.3) by a direct method (matrix-vector multiplication) is proportional to  $O(N^2)$  operations, since for small  $N$  the matrix  $\mathbf{L}^{-1}$  is dense.

Therefore, due to the complexity of solving (4.3), we are led to seek a new basis in which the

number of operations to solve the corresponding sparse linear systems may be reduced.

It turns out that a wavelet basis is well suited for a such case because we may take advantage of certain properties that wavelets possess. These properties are the sparse representation of the Green's function ( $\mathcal{L}^{-1}$ ), and the reduction of the condition number. Then we project (4.3) into the wavelet domain. The matrix  $\mathbf{L}^{-1}$  is sparse in the wavelet basis and has only  $O(N)$  entries, so solving (4.3) may require less computational effort or few number of iterative steps when an iterative method is used.

Hence, we focus on the construction of the matrix  $\mathbf{L}^{-1}$ , and consequently we shall obtain an  $O(N)$  procedure for solving (4.3). We observe that, if the entries of the vector  $\mathbf{f}$  are values of a smooth and nonoscillatory function then the wavelet transform of the vector  $\mathbf{f}$  is sparse. Therefore, the complexity is proportional to the number of the entries of the vector  $\mathbf{f}$ .

We consider the periodized version of the matrix  $\mathbf{L}$  in order to use the diagonal preconditioning available in the wavelet basis, that is

$$\mathbf{L}_p = \mathbf{L} + \mathbf{A}, \quad (4.4)$$

where  $u_{-1} = u_{N-1}$ ,  $u_N = u_0$ , and

$$\mathbf{A} = \begin{pmatrix} 0 & 0 & 0 & \cdots & 0 & 0 & a_{-1/2} \\ 0 & 0 & 0 & \cdots & 0 & 0 & 0 \\ \vdots & \vdots & \vdots & \ddots & \vdots & \vdots & \vdots \\ 0 & 0 & 0 & \cdots & 0 & 0 & 0 \\ a_{N-1/2} & 0 & 0 & \cdots & 0 & 0 & 0 \end{pmatrix}$$

Using the preconditioned matrix  $\mathbf{P}$  we require (see[2])  $\kappa(\mathbf{P L P}) < \kappa(\mathbf{L})$ , where  $\kappa$  denotes the condition number and it is defined by  $\kappa(\mathbf{L}) = \|\mathbf{L}\|_2 \|\mathbf{L}^{-1}\|_2$ . In other words,  $\kappa$  is a measure of the difficulty of solving a linear system in the sense that systems with small condition numbers are easy to solve.

Note that in the ordinary domain the condition number of the periodized matrix  $\mathbf{L}_p$  grows as  $N^2$  (Figure 4.1), and its inverse  $\mathbf{L}_p^{-1}$  is dense ( $O(N^2)$  significant entries).

However, by projecting  $\mathbf{L}_p$  into the wavelet domain, and using the periodized wavelets and the diagonal preconditioning, we obtain a small condition number which is independent of the size of



the matrix  $\mathbf{L}$ , that is,

$$\mathbf{L}^w = \mathbf{L}_p^w - \mathbf{A}^w \quad (4.5)$$

where

$$\mathbf{L}_p^w = \mathcal{W}\mathbf{L}_p\mathcal{W}^T \quad \text{and} \quad \mathbf{A}^w = \mathcal{W}\mathbf{A}\mathcal{W}^T.$$

We obtain in the last column of  $\mathbf{L}_p^w$  a zero column, since the sum of the entries in the rows of  $\mathbf{L}_p$  are identically zero. Thus the construction of  $(\mathbf{L}_p^w)^{-1}$  is reduced to finding the matrix  $\mathbf{B}^{-1}$  of the sparse matrix  $\mathbf{B}$  of size  $(N-1) \times (N-1)$  (Figure 4.2, 4.3)

$$\mathbf{L}_p^w = \begin{pmatrix} \mathbf{B} & 0 \\ c^T & 0 \end{pmatrix}$$

where  $c^T$  is a vector of length  $(N-1)$  [2].

Since the matrix  $\mathcal{W}$  is orthogonal the condition number does not change after transformation. We then apply preconditioning to the matrix  $\mathbf{B}$  in order to use a fast algorithm to compute its inverse.

The preconditioner that we use is a diagonal matrix of size  $N = 2^n$  with powers of 2 on the diagonal, that is,

$$\mathbf{P} = \text{diag}(\underbrace{2, \dots, 2}_{2^{n-1}}, \underbrace{2^2, \dots, 2^2}_{2^{n-2}}, \dots, \underbrace{2^i, \dots, 2^i}_{2^{n-i}}, \dots, \underbrace{2^{n-2}, 2^{n-2}, 2^{n-2}, 2^{n-2}}_{2^2}, \underbrace{2^{n-1}, 2^{n-1}}_2, \underbrace{2^n, 2^n}_2).$$

For simplicity we consider two cases, where  $a(x) = 1$  and  $b(x) = 0$  in  $(0, 1)$  so that  $\mathcal{L} = \frac{d^2}{dx^2}$ , then we have

$$\mathbf{L}_p = \begin{pmatrix} -2 & 1 & 0 & \cdots & 0 & 0 & 1 \\ 1 & -2 & 1 & \cdots & 0 & 0 & 0 \\ \vdots & \vdots & \vdots & \ddots & \vdots & \vdots & \vdots \\ 0 & 0 & 0 & \cdots & 1 & -2 & 1 \\ 1 & 0 & 0 & \cdots & 0 & 1 & -2 \end{pmatrix} \quad (4.6)$$

and  $a(x) = 25$ ,  $b(x) = x$  so that  $\mathcal{L} = 25\frac{d^2}{dx^2} - xu$  and

$$\mathbf{L}_p = \text{tridiag}(25, -(50 + h^2x_i), 25).$$



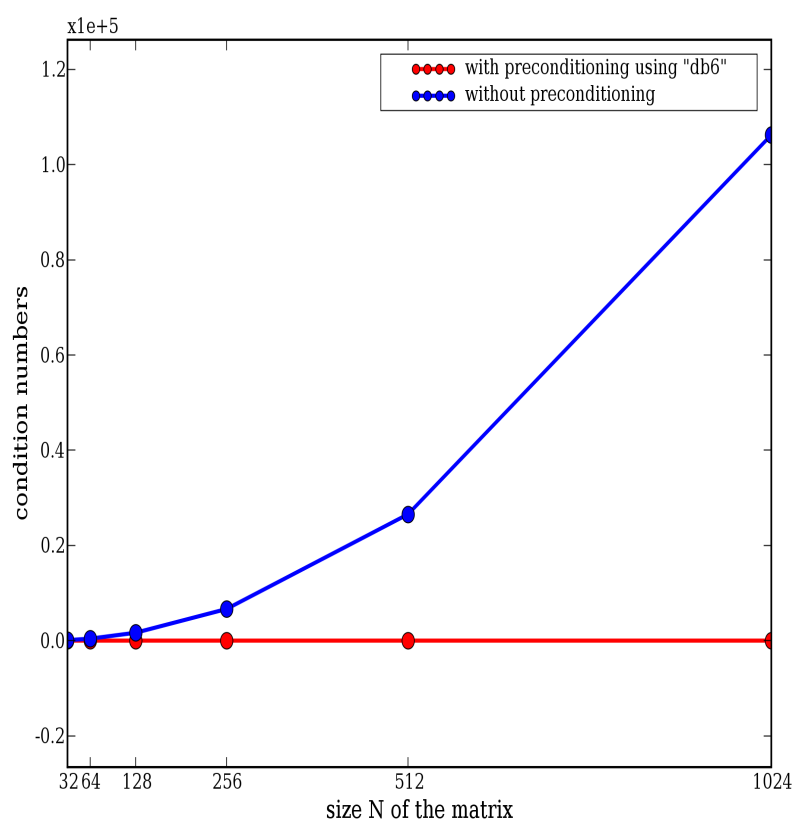


Figure 4.1: Condition numbers of the periodized matrix  $L_p$ . "db6" denotes Daubechies wavelet with six vanishing moments.

## 4.2 Numerical examples

The following table shows the condition numbers of the periodized operator with and without preconditioning ( $\kappa$  and  $\kappa_p$ , respectively). Daubechies wavelets of order 3, 4, 6, 8 are used. The size of the matrix is denoted by  $N$ . We see from the table that, when preconditioning is applied to the periodized operator, we obtain a small condition number which is independent of the size of the matrix.

$N$	Wavelet	$\mathcal{L} = \frac{d^2}{dx^2}$		$\mathcal{L} = 25 \frac{d^2}{dx^2} - xu$	
		$\kappa$	$\kappa_p$	$\kappa$	$\kappa_p$
32	db3	104.08686892	8.02083290291	104.043240437	8.02211483606
	db4	104.08686892	6.30798342451	104.043240437	6.30956620515
	db6	104.08686892	5.20017272015	104.043240437	5.20241213794
	db8	104.08686892	4.97423356654	104.043240437	4.97675725287
64	db3	415.345062232	9.08587054849	415.169154784	9.08709099872
	db4	415.345062232	6.69757750831	415.169154784	6.6988678163
	db6	415.345062232	5.26102790865	415.169154784	5.26339375318
	db8	415.345062232	4.99211875275	415.169154784	4.9942571985
128	db3	1660.37964629	10.0190304761	1659.67411095	10.0201509574
	db4	1660.37964629	6.99091581394	1659.67411095	6.99200803315
	db6	1660.37964629	5.2896859456	1659.67411095	5.29207547968
	db8	1660.37964629	4.99713668702	1659.67411095	4.9991808665
256	db3	6640.51843456	10.8406237476	6637.693347357	10.8416248698
	db4	6640.51843456	7.21876831239	6637.693347357	7.2197103613
	db6	6640.51843456	5.30351150757	6637.693347357	5.30587982655
	db8	6640.51843456	4.99850930464	6637.693347357	5.00055167315

The following proposition enables us to construct the inverse of matrices.

**Proposition 4.1.** *Consider the sequence of matrices  $X_k$ ,  $X_{k+1} = 2X_k - X_k A X_k$  with  $X_0 = \alpha A^*$ , where  $A^*$  is the adjoint matrix and  $\alpha$  is chosen so that the largest eigenvalue of  $A^* A$  is less than two. Then the sequence  $X_k$  converges to the generalized inverse  $A^\dagger$  (see [4]).*

Using the Proposition 4.1, we compute the inverse of the matrix  $\mathbf{B}_p = \mathbf{PBP}$  rescaled by a diagonal matrix  $\mathbf{P}$  which is done in  $O(N \log \kappa)$  operations. We perform the computation of the inverse until the condition  $\|\mathbf{B}_p X_k - I\| < \epsilon$  is satisfied, thus  $\mathbf{B}^{-1}$  is obtained by computing  $\mathbf{PB}_p^{-1}\mathbf{P}$ .

$\mathcal{L} = \frac{d^2}{dx^2}, \epsilon = 10^{-9}$ and db3			
$N$	$\mathbf{B}_p^{-1}$	$\mathbf{B}^{-1}$	$\mathbf{L}^{-1}$
31	10	17	21
63	10	21	25
127	11	25	29
255	11	29	33

The above table shows the number of iterations needed for computing respectively the inverses  $\mathbf{B}_p^{-1}$ ,  $\mathbf{B}^{-1}$  and  $\mathbf{L}^{-1}$ . By using wavelets of higher order, we can reduce the number of iterations needed for computing the inverse  $\mathbf{B}_p^{-1}$ .

Note from (4.5), we have

$$(\mathbf{L}^w)^{-1} = (I - (\mathbf{L}_p^w)^{-1}\mathbf{A}^w)^{-1}(\mathbf{L}_p^w)^{-1}. \quad (4.7)$$

The relation (4.7) can be computed using the Proposition 4.1.

We illustrate how a wavelet basis can be used for solving an evolution equation.

Consider the heat equation on the unit interval

$$u_t = \nu u_{xx}, \quad 0 \leq x \leq 1, \quad 0 \leq t \leq 1, \quad (4.8)$$

for  $\nu > 0$ , with the initial condition

$$u(x, 0) = u_0(x), \quad 0 \leq x \leq 1, \quad (4.9)$$

and the periodic boundary condition  $u(0, t) = u(1, t)$ .

Due to stability concerns, we choose an implicit finite difference method, where there is no restriction on the time step.

Using the method of lines, we discretize the spatial domain according to  $x_i = ih$ ,  $i = 1, \dots, N$ ,  $h = \frac{1}{N}$  and we also approximate the second derivative at  $x_j$  by

$$u_{xx}|_{x_j} \simeq \frac{u_{j+1} - 2u_j + u_{j-1}}{h^2}.$$

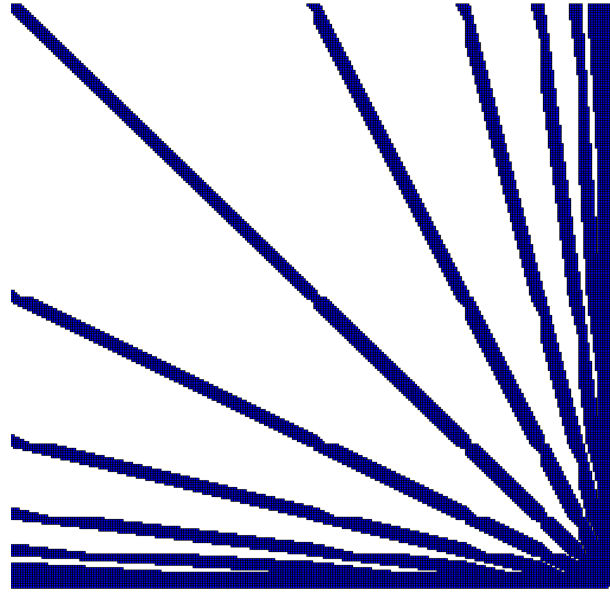


Figure 4.2: Sparsity pattern of the matrix  $\mathbf{B}$  obtained by using 'db3' and setting to zero entries with the absolute value less than  $10^{-14}$ .

Thus (4.8) is approximated by a system of ordinary differential equations

$$\frac{d\mathbf{u}}{dt} = \nu \frac{1}{h^2} \mathbf{L}\mathbf{u}, \quad (4.10)$$

where  $\mathbf{u} = (u_1, u_2, \dots, u_N)^T$  and  $u_i = u(x_i, t)$  and  $\mathbf{L}$  is a matrix identical to  $\mathbf{L}_p$  in (4.6).

Applying the trapezoidal rule to (4.10) in time, we obtain the Crank-Nicholson method that is

$$\mathbf{u}^{(n+1)} - \mathbf{u}^{(n)} = \nu \frac{h_t}{2h^2} (\mathbf{L}\mathbf{u}^{(n+1)} + \mathbf{L}\mathbf{u}^{(n)}),$$

where  $h_t$  is the time step. Rearranging we have

$$\left(\mathbf{I} - \nu \frac{h_t}{2h^2} \mathbf{L}\right) \mathbf{u}^{(n+1)} = \left(\mathbf{I} + \nu \frac{h_t}{2h^2} \mathbf{L}\right) \mathbf{u}^{(n)}. \quad (4.11)$$

Observe that, the solution of (4.11) in the ordinary domain is obtained by solving at each time the tridiagonal system. As mentioned earlier the inverse of the tridiagonal matrices are dense. However we may avoid this situation by projecting the equation into the wavelet domain.

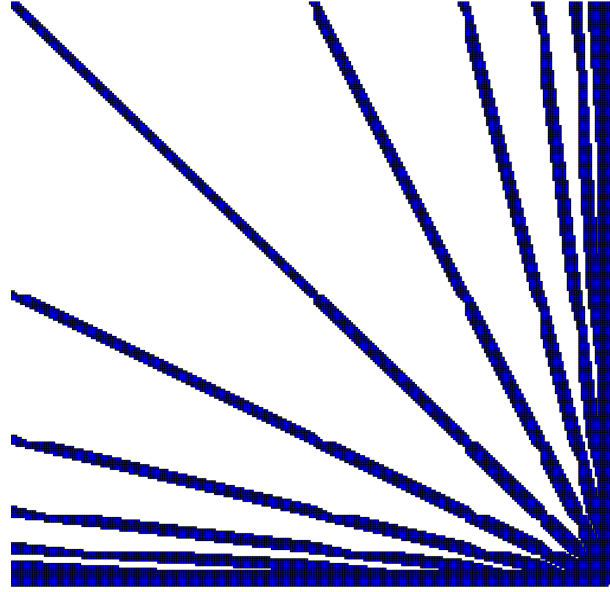


Figure 4.3: Sparsity pattern of the matrix  $\mathbf{B}^{-1}$  computing via the iterative algorithm, entries with the absolute value greater than  $10^{-9}$  are shown in blue.

We denote by  $A$  and  $B$  the tridiagonal matrices given by

$$A = \text{tridiag} \left( -\nu \frac{h_t}{2h^2}, 1 + \nu \frac{h_t}{h^2}, -\nu \frac{h_t}{2h^2} \right)$$

and

$$B = \text{tridiag} \left( \nu \frac{h_t}{2h^2}, 1 - \nu \frac{h_t}{h^2}, \nu \frac{h_t}{2h^2} \right).$$

Then the wavelet bases equation (4.11) becomes

$$\hat{\mathbf{u}}^{(n+1)} = \mathbf{C} \hat{\mathbf{u}}^{(n)}, \quad \text{where } \hat{\mathbf{u}} = \mathcal{W} \mathbf{u},$$

and

$$\mathbf{C} = (\mathcal{W} A \mathcal{W}^T)^{-1} \mathcal{W} B \mathcal{W}^T. \quad (4.12)$$

Thus the implicit scheme (4.11) is converted to an easier scheme (4.12), which is an advantage because we do not need to solve a linear system at each time. Moreover, solving (4.12) requires



Figure 4.4: Sparsity pattern of the matrix  $(\mathbf{L}^w)^{-1}$  computing via the iterative algorithm, entries with the absolute value greater than  $10^{-8}$  are shown in blue.

only  $O(N)$  operations.

We may also use the preconditioned matrix defined above to reduce number of operations.

**Remark 4.1.** The sparsity pattern of the matrix  $\mathbf{C}$  is similar to the sparsity pattern of the matrix  $\mathbf{B}$  given in Figure 4.2.

# 5. Ordinary Differential Equations

In this section we describe the wavelets efficiency to solve ordinary differential equations. The wavelet method in numerical analysis offers several advantages. One of these advantages is the representation of the solution at different scales. Before our discussion on the application of wavelets to PDE's, let us recall briefly the *weighted residuals method*.

## 5.1 The Weighted Residuals Method

Consider the following problem

$$\mathcal{L}u(x) = f(x) \quad (5.1)$$

with boundary conditions  $u(a) = a_1$  and  $u(b) = b_1$ , where  $\mathcal{L}$  is a linear differential operator

An approximation of the solution  $u$  of (5.1) can be expanded in terms of basis functions  $\phi_j$  as

$$\tilde{u}(x) = \sum_{j=0}^K c_j \phi_j(x), \quad (5.2)$$

where  $c_j$ 's are constants.

Substituting (5.2) in (5.1), we form the residual

$$R(x, c) = \mathcal{L}\tilde{u} - f, \quad (5.3)$$

which is generally not equal to zero and  $R$  depends on the  $c_j$ 's which are represented by the vector  $c$  in (5.3). We are then led to select the undetermined coefficients  $c_j$  in such a way that the residual is forced to be zero in some average sense. This can be accomplished by selecting a set of *test functions*  $w_j$  and setting the inner product of the residual  $R(x, c)$  to be zero, that is

$$\langle w_j, R \rangle = \int_a^b w_j(x) R(x, c) dx = 0, \quad j = 0, 1, \dots, K. \quad (5.4)$$

Depending on the choice of the weight functions  $w_j$  we have two methods which we elaborate on next.

### 5.1.1 Galerkin's Method

Here the test functions are chosen to be the basis functions, that is,  $w_j = \phi_j$ , we then have

$$\begin{aligned}\langle \phi_j, R \rangle &= \int_a^b \phi_j(x)(\mathcal{L}\tilde{u} - f)dx, \\ &= \sum_k c_k \int_a^b (\phi_j(x)\mathcal{L}\phi_k(x) - f(x)\phi_j(x)) dx.\end{aligned}$$

Since equation (5.4) is satisfied, we get

$$\sum_k c_k \int_a^b \phi_j(x)\mathcal{L}\phi_k(x)dx = \int_a^b f(x)\phi_j(x)dx, \quad (5.5)$$

which can be written in matrix form as

$$Ac = b,$$

with

$$A_{j,k} = \int_a^b \phi_j(x)\mathcal{L}\phi_k(x)dx, \text{ and } b_j = \int_a^b f(x)\phi_j(x)dx.$$

### 5.1.2 The Collocation Method

Here the test function is chosen to be the *shifted Dirac delta function*

$$w_j(x) = \delta(x - x_j), \quad (5.6)$$

where the shifted Dirac delta function satisfies

$$\delta(x - x_j) = \begin{cases} 1 & x = x_j, \\ 0 & \text{otherwise,} \end{cases} \quad (5.7)$$

and has the property

$$\int f(x)\delta(x - x_j)dx = f(x_j)$$

and  $x_j$  denotes a point in  $[a, b]$ .

Substituting (5.6) in (5.4) yields

$$\begin{aligned}\langle \delta(x - x_j), R \rangle &= \int_a^b \delta(x - x_j)(\mathcal{L}\tilde{u} - f)dx, \\ &= \sum_k c_k \int_a^b (\delta(x - x_j)\mathcal{L}\phi_k(x) - f(x)\delta(x - x_j)) dx.\end{aligned}$$



So we obtain

$$\begin{aligned}\sum_k c_k \int_a^b \delta(x - x_j) \mathcal{L}\phi_k(x) dx &= \int_a^b f(x) \delta(x - x_j) dx, \\ \sum_k c_k \mathcal{L}\phi_k(x_j) &= f(x_j).\end{aligned}$$

## 5.2 Wavelet Galerkin Method

We follow Amaratunga *et al.*'s method for solving differential equations as described in [29], but we use the convention of decreasing subspaces of I. Daubechies and S. Mallat (see [16]).

We consider problem (5.1) with some slight changes. We assume that  $u$  and  $f$  are both periodic with period  $d$ , that is

$$\begin{aligned}u(0) &= u(d), \\ f(0) &= f(d).\end{aligned}$$

The wavelet-Galerkin approximation to the solution  $u(x)$  at scale  $m$  is

$$u(x) = 2^{-m/2} \sum_{k=0}^{2^{-m}d-1} \tilde{c}_k \varphi(2^{-m}x - k), \quad (5.8)$$

where  $\tilde{c}_k = \langle u, \varphi_{m,k} \rangle$ .

In order to perform the computation, one idea is to express the approximate solution as a convolution of two vectors, therefore the transformation from wavelet space to physical space is then accomplished by the FFT.

We begin by making the substitution  $y = 2^{-m}x$ . We have

$$U(y) = u(x) = \sum_{k=0}^{2^{-m}d-1} c_k \varphi(y - k), \quad \text{with } c_k = 2^{-m/2} \tilde{c}_k. \quad (5.9)$$

Since  $u$  is periodic with period  $d$ , it implies  $U(y)$  is also periodic with period  $2^{-m}d \in \mathbb{Z}$ . Likewise  $c_k$  has period  $2^{-m}d$ .

Now, by letting  $y$  take only integer values, we are ensured to have all the values of  $u(x)$  at the

dyadic points  $x = 2^m y$ . We discretize  $U(y)$ , that is,

$$\begin{aligned} U_i = U(i) &= \sum_{k=0}^{2^m d - 1} c_k \varphi(i - k), \\ &= \sum_{k=0}^{2^m d - 1} c_k \varphi_{i-k}, \quad i = 0, 1, 2, \dots, 2^m d - 1, \end{aligned}$$

where we use the notation  $\varphi_{i-k} := \varphi(i - k)$ .

We therefore express  $U$  as a convolution, i.e.

$$U = K_\varphi * c, \quad (5.10)$$

where  $K_\varphi$  is the first column of a matrix having entries  $\varphi_{i-k}$ , and  $c = (c_0, c_1, \dots, c_{2^m d - 1})^T$ .

Since the Fourier transform of a convolution of two vectors is a multiplication component by component of the discrete Fourier transform of the vectors, equation (5.10) may be written as

$$\hat{U} = \hat{K}_\varphi \cdot \hat{c}, \quad (5.11)$$

where  $\cdot$  denotes pointwise multiplication.

Similarly, we define

$$F(y) = f(x) = \sum_{k=0}^{2^m d - 1} g_k \varphi(y - k), \quad g_k = 2^{-m/2} \tilde{g}_k, \quad (5.12)$$

where  $g_k$  is also periodic.

Discretizing  $F(y)$  we then rewrite (5.12) as

$$F_i = \sum_{k=0}^{2^m d - 1} g_k \varphi_{i-k}. \quad (5.13)$$

Equation (5.13) is written as a convolution

$$F = K_\varphi * g,$$

with  $g = (g_0, g_1, \dots, g_{2^m d - 1})^T$ .

Taking the Fourier transform of both sides of (5.2), we get

$$\hat{F} = \hat{K}_\varphi \cdot \hat{g}. \quad (5.14)$$

Now applying Galerkin's method (5.5), we get

$$\begin{aligned} \sum_{k=0}^{2^{-m}d-1} c_k \int_{\mathbb{R}} \varphi(y-j) \mathcal{L}\varphi(y-k) dy &= \sum_{k=0}^{2^{-m}d-1} g_k \int_{\mathbb{R}} \varphi(y-k) \varphi(y-j) dy, \\ \sum_{k=0}^{2^{-m}d-1} c_k \int_{\mathbb{R}} \varphi(y'-(j-k)) \mathcal{L}\varphi(y') dy' &= \sum_{k=0}^{2^{-m}d-1} g_k \delta_{k,j}, \quad (y' = y - k) \\ \sum_{k=0}^{2^{-m}d-1} c_k r_{j-k} &= g_j, \quad j = 0, 1, \dots, 2^{-m}d - 1, \end{aligned} \quad (5.15)$$

where  $r_{j-k}$  is the same as defined in (3.25) in Chapter 3.

Equation (5.15) can be written as a convolution

$$K_r * c = g. \quad (5.16)$$

Taking the Fourier transform of (5.16), we have

$$\hat{K}_r \cdot \hat{c} = \hat{g}. \quad (5.17)$$

We can then solve the problem by combining (5.14), (5.17) and (5.11) to get

$$\hat{U} = \hat{F} / \hat{K}_r, \quad (5.18)$$

where  $/$  denotes a pointwise division.

**Remark 5.1.**  $r_{j-k} = 0$  for  $j - k \notin [2 - L, L - 2]$ .

A usual problem in solving differential equations involves how to incorporate the boundary when dealing with arbitrary boundary conditions. There are several techniques to handle this situation. One can either use *Lagrange multipliers* or the *capacitance matrix* [28]. In our case we focus on the latter method.

We consider problem (5.1) again with  $0 < a < b < d$ ,  $d \in \mathbb{Z}$ , and  $u(x)$ ,  $f(x)$  functions of period  $d$ . Let  $u(x) = v(x) + w(x)$ , such that

$$\begin{cases} \mathcal{L}v(x) = f(x), & x \in (a, b), \\ v(0) = v(d), \end{cases} \quad (5.19)$$

and

$$\begin{cases} \mathcal{L}w(x) = 0, & x \in (a, b), \\ \mathcal{L}w(x) = X(x), & x \in (0, d), \end{cases} \quad (5.20)$$

where

$$X(x) = X_a\delta(x - a) + X_b\delta(x - b)$$

and  $\delta(x)$  is the *Dirac delta function*. We must find constants  $X_a$  and  $X_b$  such that the boundary conditions for  $u$  are satisfied at  $a$  and  $b$ .

To this end, we introduce the *Green's function*  $G(x)$  of the differential equation which is given by

$$\begin{cases} \mathcal{L}G(x) = \delta(x), \\ G(0) = G(d). \end{cases} \quad (5.21)$$

Also (see [29])

$$w(x) = X_aG(x - a) + X_bG(x - b). \quad (5.22)$$

Since (5.19) and (5.21) are periodic boundary problems, we solve them easily by following the procedure outlined above for periodic boundary conditions. It remains just to find  $X_a$  and  $X_b$  given by

$$\begin{aligned} w(a) &= X_aG(0) + X_bG(a - b) = a_1 - v(a), \\ w(b) &= X_aG(b - a) + X_bG(0) = b_1 - v(b), \end{aligned}$$

so

$$\begin{bmatrix} G(0) & G(a - b) \\ G(b - a) & G(0) \end{bmatrix} \begin{bmatrix} X_a \\ X_b \end{bmatrix} = \begin{bmatrix} a_1 - v(a) \\ b_1 - v(b) \end{bmatrix} \quad (5.23)$$

Hence we get the solution  $u$  by adding the solution  $w$  obtained after solving (5.23) and (5.19).

Due to the fact that the Dirac delta function and the scaling function have the same compact support in the wavelet domain, solving (5.21) may present some problems which can be avoided by introducing offset boundary sources.

Let  $s$  be the offset. We have

$$\alpha = a - s, \quad \beta = b + s,$$

where  $L/2^{-m} < s < \max(a, d - b)$ . Then

$$X(x) = X_a\delta(x - \alpha) + X_b\delta(x - \beta)$$

and  $X_a$  and  $X_b$  are determined from

$$\begin{bmatrix} G(a - \alpha) & G(a - \beta) \\ G(b - \alpha) & G(b - \beta) \end{bmatrix} \begin{bmatrix} X_a \\ X_b \end{bmatrix} = \begin{bmatrix} a_1 - v(a) \\ b_1 - v(b) \end{bmatrix} \quad (5.24)$$

By transforming the problem (5.1) to a convolution problem (5.16), and using the FFT enables us to obtain the solution in  $O(N \log_2 N)$  operations.

### 5.3 Wavelet Collocation Method

Here, we follow Bertoluzza and Naldi's approach [1] for solving problem (5.1). This approach is based on the use of the *autocorrelation function*  $\theta$  of Debauchie's compactly supported wavelets. We define the autocorrelation function  $\theta$  as

$$\theta(x) = \int_{\mathbb{R}} \varphi(y) \varphi(y - x) dy, \quad (5.25)$$

Due to the orthonormality property of the set  $\{\varphi(x - k), k \in \mathbb{Z}\}$ , the autocorrelation function  $\theta$  satisfies the *interpolation property*

$$\theta(n) = \begin{cases} 1 & \text{if } n = 0, \\ 0 & \text{otherwise.} \end{cases} \quad (5.26)$$

It can be shown by integration by parts for integers  $l$  and  $s$  satisfying  $0 \leq l \leq s$ , that we have

$$\theta^{(s)}(x) = (-1)^{s-l} \int_{\mathbb{R}} \varphi^{(l)}(y) \varphi^{(s-l)}(y - x) dy. \quad (5.27)$$

In the same manner as the scaling function, the autocorrelation function generates also a MRA, unfortunately which is non-orthonormal.

We denote by  $\check{V}_j$  the subspace spanned by  $\{\theta_{j,k}(x) = 2^{-j/2} \theta(2^{-j}x - k), k \in \mathbb{Z}\}$ .

To solve problem (5.1), the approximate solution  $u_j \in \check{V}_j$  is written in terms of its values at the dyadic points  $x_k = k2^j$ , i.e.

$$u_j(x) = \sum_{k=0}^{2^j} u_j(k2^j) \theta(2^{-j}x - k), \quad (5.28)$$

and

$$u_j(0) = a, \quad u_j(1) = b.$$

To handle the situation at the boundary points, two methods are available.

First, we may introduce the following functions

$$\tilde{\theta}_{j,0} = \sum_{k=-\infty}^0 \theta_{j,k}, \quad \tilde{\theta}_{j,2^{-j}} = \sum_{k=2^{-j}}^{+\infty} \theta_{j,k}. \quad (5.29)$$

Then (5.28) and (5.29) imply

$$u_j(x) = u_j(0)\tilde{\theta}_{j,0} + \sum_{k=1}^{2^{-j}-1} u_j(k2^j)\theta(2^{-j}x - k) + u_j(1)\tilde{\theta}_{j,2^{-j}}, \quad (5.30)$$

which satisfy the boundary conditions.

Referring to subsection 5.1.2, problem (5.1) may be written as

$$\mathcal{L}u_j(x_n) = f(x_n), \quad n = 1, \dots, 2^{-j} - 1, \quad (5.31)$$

where  $x_n = n2^j$ .

Although this method is the easier one, it produces an error  $O(2^{j/2})$ , which is computationally prohibitive.

The second method is to define the approximate solution  $u_j$  by

$$u_j(x) = \sum_{k=-L+1}^{2^{-j}+L-1} \alpha_k \theta_{j,k}. \quad (5.32)$$

Therefore, we require  $2^{-j} + 2L - 1$  collocation points. As we already have  $2^{-j} + 1$  dyadic points  $x_k = k2^j$ ,  $k = 0, \dots, 2^{-j}$ , the additional  $2L - 2$  points are placed near the boundary. For the left boundary these points are given by  $x_k = (2k + 1)2^{j+1}$ ,  $k = 0, \dots, L - 2$  and for the right boundary they are given by  $x_k = 1 - (2k + 1)2^{j+1}$ ,  $k = 0, \dots, L - 2$ . Hence we improve the convergence near the boundary points.

**Remark 5.2.** Given the definition of  $\theta$  in (5.25) and (5.27), the matrix corresponding to the linear system (5.31) is the same if we use Galerkin's method to solve the problem. Therefore, we may reduce the complexity of solving (5.31) by projecting it into the wavelet domain and use the diagonal preconditioning available for Galerkin's method.

## 5.4 Numerical Results

### 5.4.1 Amaratunga et al. Method

Consider the following ordinary differential equation

$$\begin{cases} u_{xx} + \frac{\pi^2}{4}u = \frac{\pi^2}{4}, & 0 \leq x \leq 1 \\ u(0) = 1, \quad u(1) = 0. \end{cases} \quad (5.33)$$

The exact solution is

$$u(x) = 1 - \sin\left(\frac{\pi x}{2}\right). \quad (5.34)$$

We solve the problem using Amaratunga *et al.* method described in Section 5.2 and we compare it with the finite difference method.

In Figure 5.2(a), we display the plot of the exact and approximate solution obtained by Amaratunga *et al.* method at level  $m = -6$ ,  $d = 3$ , and using Daubechies wavelets of order 3. Figure 5.2(b) shows the exact and approximate solution obtained by the finite difference method (FDM) with  $N = 2^{-m}$  (the number of points of discretization). We observe in Figure 5.1 that Amaratunga *et al.* method gives a better approximation than the finite difference method.

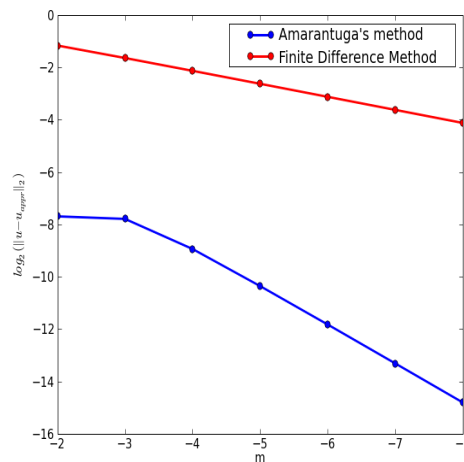
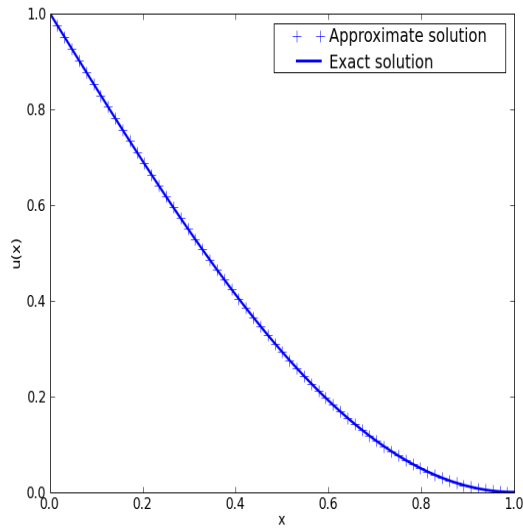
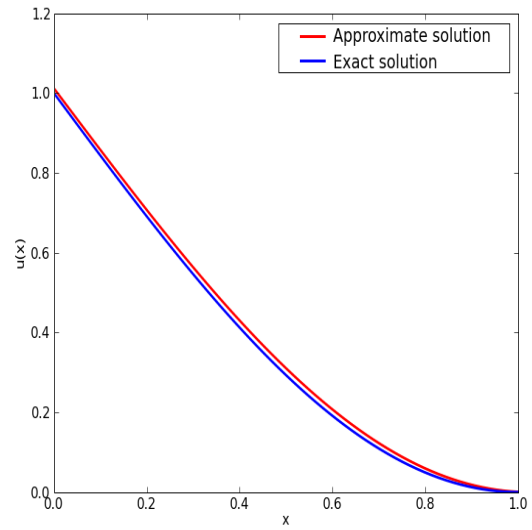


Figure 5.1:  $\log_2$  of norm-2 error of Amaratunga method and FDM.



(a) Amarantunga' method for problem (5.33)



(b) Finite Difference Method for the same problem

Figure 5.2: Exact and approximate solution

### 5.4.2 Collocation Method (Bertoluzza's Method)

To show the efficiency of the method, we consider the following problem

$$\begin{cases} u_{xx} - u = e^x, & 0 \leq x \leq 1 \\ u(0) = 1, u(1) = 0. \end{cases} \quad (5.35)$$

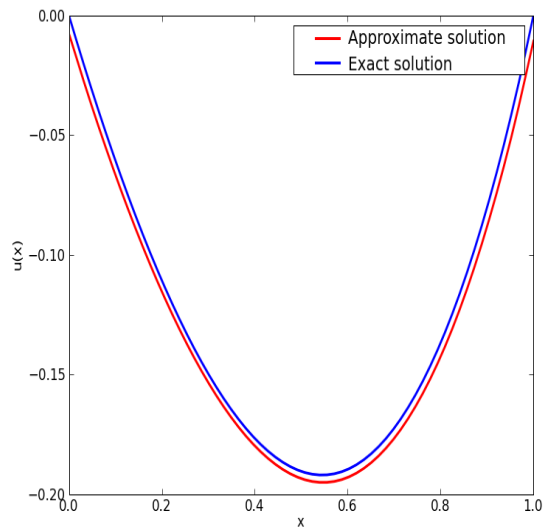
The exact solution is

$$-\frac{e^2}{2(e^2 - 1)}e^x + \frac{e^2}{2(e^2 - 1)}e^{-x} + \frac{1}{2}xe^x. \quad (5.36)$$

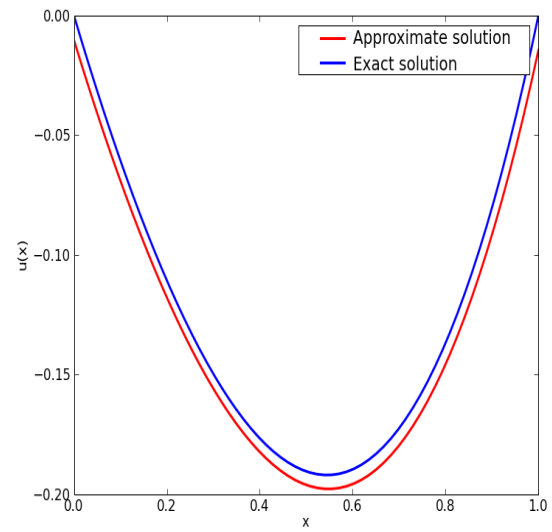
We compare the collocation method with the finite difference method again .

Figure 5.3(a) shows the approximate solution computed at level  $m = -6$  using Daubechies wavelet of order 3 and the exact solution. Figure 5.3(b) is the plot of the same problem computed using the finite difference method. The norm of the error is shown in Figure 5.3(c).

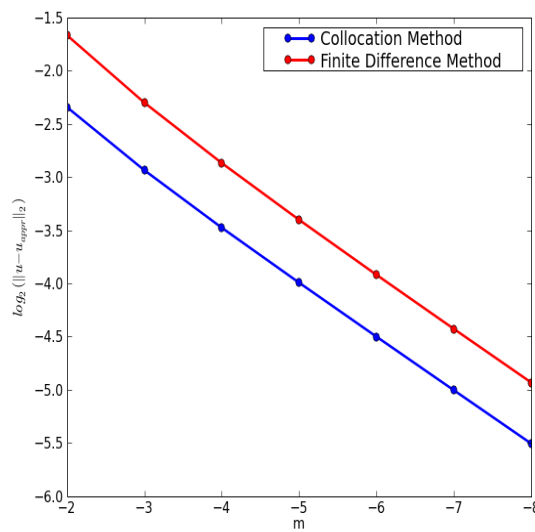




(a) Collocation Method for problem (5.35)



(b) Finite Difference Method for the same problem



(c) log<sub>2</sub> norm-2 error of Collocation and Finite Difference Method

Figure 5.3: Exact and approximate solution

Let us consider

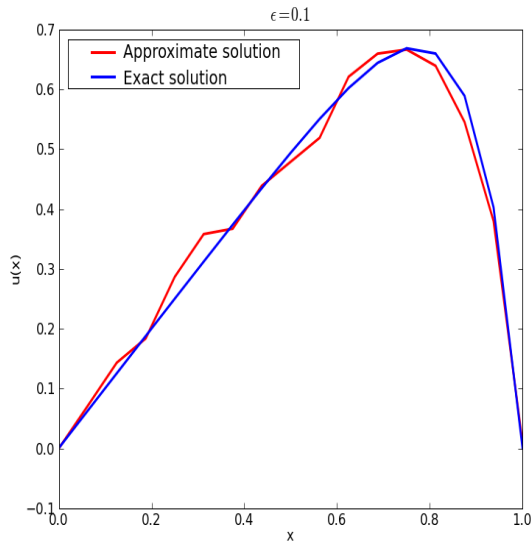
$$\begin{cases} -\epsilon u_{xx} + u_x = 1, & 0 \leq x \leq 1 \\ u(0) = 1, u(1) = 0. \end{cases} \quad (5.37)$$

The exact solution is

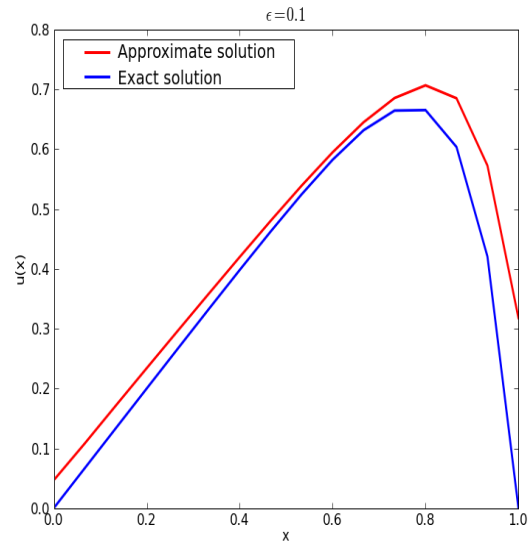
$$-\epsilon \left( -\frac{1}{\epsilon}x + \frac{1}{\epsilon(1 - e^{\frac{1}{\epsilon}})} - \frac{1}{\epsilon(1 - e^{\frac{1}{\epsilon}})}e^{\frac{1}{\epsilon}x} \right). \quad (5.38)$$

We use problem (5.37) to compare the accuracy of the three methods, Bertoluzza, Amaratunga and finite difference method. For this purpose, we choose  $\epsilon = 0.1$ , and we use Daubechies wavelet having three vanishing moments.

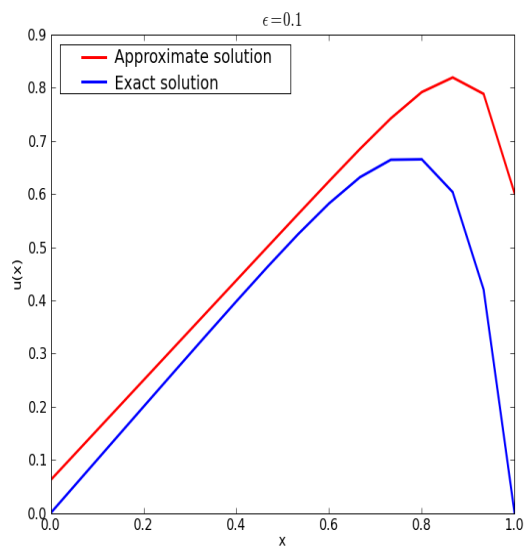
For  $\epsilon = 0.1$ , Figure 5.4 shows the plots of the exact and approximate solution of the three methods. In Figure 5.4(d) Daubechies wavelet of order 6 is used. We clearly notice that Amaratunga's method is the most accurate



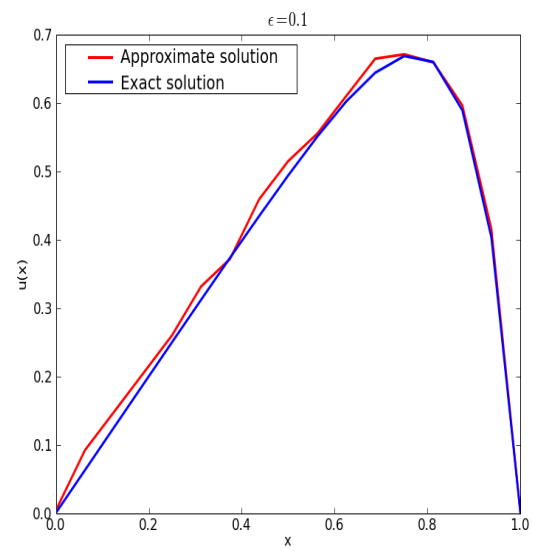
(a) Amaratunga's method



(b) Bertoluzza's method



(c) finite difference method



(d) Amaratunga's method

Figure 5.4: The exact and the approximate solution computed at scale  $m = -4$

## 6. Partial Differential equations

In this section, we are solving the evolution equation

$$\begin{cases} u_t = \mathcal{L}u + \mathcal{N}u, \\ u(0, t) = u(1, t), \quad t \in [0, T], \\ u(x, 0) = u_0(x), \quad x \in [0, 1], \end{cases} \quad (6.1)$$

where the operators  $\mathcal{L}$  and  $\mathcal{N}$  are time independent, and they represent the linear part and the nonlinear part of the equation respectively.

We Follow Beylkin's approach ([8], [7], [21]). We solve problem (6.1) using the semigroup approach. The semigroup method enables us to convert a partial differential equation to a nonlinear integral equation given by

$$u(x, t) = e^{t\mathcal{L}}u_0(x) + \int_0^t e^{(t-\tau)\mathcal{L}}\mathcal{N}u(x, \tau)d\tau. \quad (6.2)$$

### 6.1 Numerical Quadrature

A more general form of (6.2) is given by

$$u(x, t) = e^{(t-\eta)\mathcal{L}}u(x, \eta) + \int_0^t e^{(t-\tau)\mathcal{L}}\mathcal{N}u(x, \tau)d\tau, \quad (6.3)$$

where  $0 \leq \eta \leq t$ .

Discretizing equation (6.3) for a fixed time mesh of width  $\Delta t$  and taking  $\eta = t_{n+1-l}$  gives the numerical quadrature for the integral equation (6.3)

$$u_{n+1} = e^{l\Delta t\mathcal{L}}u_{n+1-l} + \Delta t \left( \gamma N_{n+1} + \sum_{m=0}^{M-1} \beta_m N_{n-m} \right), \quad (6.4)$$

where  $t_n = n\Delta t$ ,  $u_n \equiv u(x, t_n)$ ,  $N_n \equiv \mathcal{N}u(x, t_n)$ ,  $l \leq M$ ,  $M$  is the number of time steps used in the approximation of the integral, and  $\gamma = \gamma(l, \Delta\mathcal{L})$  and  $\beta_m = \beta_m(l, \Delta\mathcal{L})$  are the operator coefficients dependent on  $l$ .

Thus, if  $\gamma = 0$  the algorithm (6.4) is explicit and it is implicit otherwise. This family of schemes

is referred to as the *Exact Linear Part* (ELP) [9].

Now we focus our discussion on how to find the coefficients  $\gamma$  and  $\beta_m$  of (6.4). We start by expanding  $u_{n+1}$  in the Taylor series at the time level  $t_{n+1-l}$

$$u_{n+1} = \sum_{k=0}^{\infty} u_{n+1-l}^{(k)} \frac{(l\Delta t)^k}{k!}, \quad (6.5)$$

where

$$u_{n+1-l}^{(k)} = \left. \frac{\partial^k}{\partial t^k} u(t) \right|_{t=t_{n+1-l}}.$$

By (6.1) we have

$$\begin{aligned} u^{(1)} &= \mathcal{L}u + N, \\ u^{(2)} &= \mathcal{L}u^{(1)} + N^{(1)} = \mathcal{L}^2u + \mathcal{L}N + N^{(1)}, \\ u^{(3)} &= \mathcal{L}^2u^{(1)} + \mathcal{L}N^{(1)} + N^{(2)} = \mathcal{L}^3u + \mathcal{L}^2N + \mathcal{L}N^{(1)} + N^{(2)}, \\ &\dots \end{aligned} \quad (6.6)$$

$$u^{(k)} = \mathcal{L}^k u + \sum_{j=0}^{k-1} N^{(j)} \mathcal{L}^{k-1-j}. \quad (6.7)$$

Substituting (6.7) into (6.5), we have

$$\begin{aligned} u_{n+1} &= \sum_{k=0}^{\infty} \frac{(l\Delta t)^k}{k!} \left( \mathcal{L}^k u_{n+1-l} + \sum_{j=0}^{k-1} \mathcal{L}^{k-1-j} N_{n+1-l}^{(j)} \right), \\ &= \sum_{k=0}^{\infty} \mathcal{L}^k u_{n+1-l} \frac{(l\Delta t)^k}{k!} + \sum_{k=0}^{\infty} \sum_{j=0}^{k-1} \mathcal{L}^{k-1-j} N_{n+1-l}^{(j)} \frac{(l\Delta t)^k}{k!}, \end{aligned} \quad (6.8)$$

$$= e^{l\Delta t \mathcal{L}} u_{n+1-l} + \sum_{k=0}^{\infty} \sum_{j=0}^k \mathcal{L}^{k-j} N_{n+1-l}^{(j)} \frac{(l\Delta t)^{k+1}}{(k+1)!}. \quad (6.9)$$

Changing the order of summation of the second term in (6.9), we obtain

$$\begin{aligned} \sum_{k=0}^{\infty} \sum_{j=0}^k \mathcal{L}^{k-j} N_{n+1-l}^{(j)} \frac{(l\Delta t)^{k+1}}{(k+1)!} &= \sum_{j=0}^{\infty} N_{n+1-l}^{(j)} \sum_{k=j}^{\infty} \mathcal{L}^{k-j} \frac{(l\Delta t)^{k+1}}{(k+1)!}, \\ &= \sum_{j=0}^{\infty} N_{n+1-l}^{(j)} (l\Delta t)^{j+1} \left( \frac{1}{(l\Delta t \mathcal{L})^{j+1}} \sum_{k=j+1}^{\infty} \frac{(l\Delta t \mathcal{L})^k}{k!} \right), \\ &= \sum_{j=0}^{\infty} N_{n+1-l}^{(j)} (l\Delta t)^{j+1} Q_{j+1}(l\Delta t \mathcal{L}), \end{aligned} \quad (6.10)$$

where

$$Q_j(x) := \frac{e^x - E_j(x)}{x^j} \quad (6.11)$$

and

$$E_j(x) := \sum_{k=0}^{j-1} \frac{x^k}{k!}. \quad (6.12)$$

Substituting (6.10) into (6.9), we have

$$u_{n+1} = e^{l\Delta t\mathcal{L}}u_{n+1-l} + \Delta t \sum_{j=0}^{\infty} N_{n+1-l}^{(j)} l^{j+1} (\Delta t)^j Q_{j+1}(l\Delta t\mathcal{L}). \quad (6.13)$$

Back to (6.4), we expand  $N_{n+1}$  and  $N_{n-m}$  in the Taylor series at the time level  $t_{n+1-l}$

$$N_{n+1} = \sum_{j=0}^{\infty} N_{n+1-l}^{(j)} \frac{(l\Delta t)^j}{j!}, \quad (6.14)$$

$$N_{n-m} = \sum_{k=0}^{\infty} N_{n+1-l}^{(j)} \frac{((l-m-1)\Delta t)^j}{j!}. \quad (6.15)$$

Substituting into (6.4), we have

$$\begin{aligned} u_{n+1} &= e^{l\Delta t\mathcal{L}}u_{n+1-l} + \Delta t \left( \gamma \sum_{j=0}^{\infty} N_{n+1-l}^{(j)} \frac{(l\Delta t)^j}{j!} + \sum_{m=0}^{M-1} \beta_m \sum_{j=0}^{\infty} N_{n+1-l}^{(j)} \frac{((l-m-1)\Delta t)^j}{j!} \right), \\ &= e^{l\Delta t\mathcal{L}}u_{n+1-l} + \Delta t \left[ \sum_{j=0}^{\infty} N_{n+1-l}^{(j)} \frac{\Delta t^j}{j!} \left( l^j \gamma + \sum_{m=0}^{M-1} \beta_m (l-m-1)^j \right) \right]. \end{aligned} \quad (6.16)$$

Comparing equations (6.16) and (6.13) shows

$$Q_{j+1}(l\Delta t\mathcal{L}) = \frac{1}{l^{j+1}j!} \left( l^j \gamma + \sum_{m=0}^{M-1} \beta_m (l-m-1)^j \right) \quad (6.17)$$

which holds for  $j = 0, 1, \dots, M$  in the implicit case, and  $j = 0, 1, \dots, M-1$  in the explicit case.

As an example, if we choose  $l = 1$  and  $M = 3$ , then

$$Q_{j+1}(\Delta t\mathcal{L}) = \frac{1}{j!} \left( \gamma + (-1)^j \sum_{m=0}^2 \beta_m m^j \right). \quad (6.18)$$

For  $j = 0, 1, 2, 3$ , we have

$$Q_1(\Delta t\mathcal{L}) = \gamma + \sum_{m=0}^2 \beta_m, \quad (6.19)$$

$$Q_2(\Delta t\mathcal{L}) = \gamma - 1 \sum_{m=0}^2 \beta_m m, \quad (6.20)$$

$$Q_3(\Delta t\mathcal{L}) = \frac{1}{2} \left( \gamma + \sum_{m=0}^2 \beta_m m^2 \right), \quad (6.21)$$

$$Q_4(\Delta t\mathcal{L}) = \frac{1}{6} \left( \gamma - \sum_{m=0}^2 \beta_m m^3 \right) \quad (6.22)$$

Solving (6.19) to (6.22) we get

$$\gamma = Q_2(\Delta t\mathcal{L})/3 + Q_3(\Delta t\mathcal{L}) + Q_4(\Delta t\mathcal{L})$$

$$\beta_0 = Q_1(\Delta t\mathcal{L}) + Q_2(\Delta t\mathcal{L})/2 - 2Q_3(\Delta t\mathcal{L}) - 3Q_4(\Delta t\mathcal{L})$$

$$\beta_1 = -Q_2(\Delta t\mathcal{L}) + Q_3(\Delta t\mathcal{L}) + 3Q_4(\Delta t\mathcal{L})$$

$$\beta_2 = Q_2(\Delta t\mathcal{L})/6 - Q_4(\Delta t\mathcal{L})$$

Since the coefficients of the ELP schemes are obtained in terms of the operator  $Q_j(l\Delta t\mathcal{L})$ , it is therefore necessary to perform accurately its computation and hence avoid the computation of  $(l\Delta t\mathcal{L})^{-1}$ . In [9], the authors used the method of *scaling and squaring*. They first observed that

$$Q_0(2x) = Q_0^2(x), \quad (6.23)$$

and thereafter they performed the computation of  $Q_0(2^{-n}l\Delta t\mathcal{L})$  using the Taylor expansion where  $n$  is an integer chosen so that the largest singular value of  $2^{-n}l\Delta t\mathcal{L}$  is less than one. Finally, the matrix obtained from the Taylor expansion is then squared  $n$  times to get the desired result. The same method may be applied to compute  $Q_j(l\Delta t\mathcal{L})$ ,  $j = 1, 2, \dots$ , for any finite  $j$ .

## 6.2 Evaluating Functions in Wavelet Bases

In this section, we assume that  $\mathcal{N}u \equiv \mathcal{N}f(u)$ . Therefore we are concerned with the representation of the function  $f(u)$  into the wavelet domain, where  $f$  is an analytic function. If  $u$  and  $f(u) \in V_0$ , we may write

$$u(x) = \sum_k s_k^0 \varphi(x - k), \quad (6.24)$$

and

$$f(u) = \sum_k f(s_k^0) \varphi(x - k), \quad (6.25)$$

with an additional assumption that the scaling function is interpolating so that

$$s_k^0 = u(k). \quad (6.26)$$

In what follows we show how to evaluate  $f(u)$  without considering the assumption that the scaling function is interpolating. We begin to represent  $f(u) = u^2$ , and then extend to general  $f(u)$ .

Let  $P_j u$  and  $Q_j u$  be the orthogonal projections of  $u$  into the subspaces  $V_j$  and  $W_j$  for  $j = 0, 1, 2, \dots, J \leq n$ , respectively. Let  $j_f$  be the finest scale for which  $u$  has significant wavelet coefficients (i.e., coefficients greater than some  $\epsilon$  in the  $l^\infty$ -norm). Then the projection of  $u$  may be expressed as

$$(P_0 u)_\epsilon(x) = \sum_{j=j_f}^J \sum_{\{k: |d_k^j| > \epsilon\}} d_k^j \psi_{j,k}(x) + \sum_{k \in \mathbb{F}_{2^{n-J}}} s_k^J \varphi_{J,k}(x), \quad (6.27)$$

where  $\mathbb{F}_{2^{n-J}} = \{0, 1, \dots, 2^{n-J} - 1\}$ .

The expansion of  $((P_0 u)_\epsilon)^2$  in a 'telescopic' series is given by

$$((P_0 u)_\epsilon)^2 - (P_J u)^2 = \sum_{j=j_f}^J (P_{j-1} u)^2 - (P_j u)^2. \quad (6.28)$$

Using the fact that  $P_{j-1} = P_j + Q_j$  we have

$$((P_0 u)_\epsilon)^2 = (P_J u)^2 + \sum_{j=j_f}^J 2(P_j u)(Q_j u) + (Q_j u)^2. \quad (6.29)$$

To evaluate (6.29), one needs to compute  $(P_j u)(Q_j u)$ ,  $(Q_j u)^2$ , and  $(P_J u)^2$ . However, the computation of these terms may present a difficulty due to the fact that they may not necessarily belong to the same subspace as their respective multiplicands. Therefore, we may handle this situation by using the definition of  $V_j$  and  $W_j$ , and consider  $P_j u \in V_j \subset V_{j-j_0}$  and  $Q_j u \in W_j \subset V_{j-j_0}$  for some  $j_0 \geq 1$ . Hence, for a given accuracy  $\epsilon$  and an appropriately chosen  $j_0$ ,  $(P_J u)^2$ ,  $(P_j u)(Q_j u)$ , and  $(Q_j u)^2$  belong to the same subspace  $V_{j-j_0}$ , and are evaluated using (6.25) for finite  $k$ . In order to determine  $j_0$ , we consider the case  $j = 0$  and assume that



$u \in V_0 \subset V_{-j_0}$ . Then we have

$$\begin{aligned} s_l^{-j_0} &= 2^{j_0/2} \int_{\mathbb{R}} u(x) \varphi(2^{j_0}x - l) dx, \\ &= \frac{2^{j_0/2}}{2\pi} \int_{\mathbb{R}} \hat{u}(2^{j_0}\xi) \overline{\hat{\varphi}(\xi)} e^{i\xi l} d\xi, \\ &= \frac{2^{j_0/2}}{2\pi} \sum_{k \in \mathbb{Z}} \int_{-\pi}^{\pi} \hat{u}(2^{j_0}(\xi + 2\pi k)) \overline{\hat{\varphi}(\xi + 2\pi k)} e^{i\xi l} d\xi. \end{aligned} \quad (6.30)$$

Since  $u \in V_0$ , for any  $\epsilon > 0$  there is a  $j_0$  such that the infinite sum in (6.30) may be approximated to within  $\epsilon$  by  $k = 0$  term

$$s_l^{-j_0} = \frac{2^{j_0/2}}{2\pi} \int_{-\pi}^{\pi} \hat{u}(2^{j_0}\xi) \overline{\hat{\varphi}(\xi)} e^{i\xi l} d\xi. \quad (6.31)$$

Before evaluating (6.31), we recall that a scaling function  $\varphi(x)$  has  $M$  shifted vanishing moments if and only if  $\int_{\mathbb{R}} (x - \alpha)^m \varphi(x) dx = 0$ , where  $\alpha = \int_{\mathbb{R}} x \varphi(x) dx$  [16]. Using (2.1) and taking the  $m^{\text{th}}$  partial derivative with respect to  $\xi$ , we can write

$$\begin{aligned} \frac{\partial^m}{\partial \xi^m} e^{-i\xi \alpha} \overline{\hat{\varphi}(\xi)} &= \frac{\partial^m}{\partial \xi^m} \left( \int_{\mathbb{R}} \varphi(x) e^{i\xi(x-\alpha)} dx \right), \\ &= (i)^m e^{-i\xi \alpha} \int_{\mathbb{R}} (x - \alpha)^m \varphi(x) e^{i\xi x} dx. \end{aligned} \quad (6.32)$$

Evaluating (6.32) at  $\xi = 0$ , we have

$$\int_{\mathbb{R}} (x - \alpha)^m \varphi(x) dx = \frac{1}{(i)^m} \frac{\partial^m}{\partial \xi^m} e^{-i\alpha \xi} \overline{\hat{\varphi}(\xi)} \Big|_{\xi=0} = 0,$$

so

$$\frac{1}{(i)^m} \frac{\partial^m}{\partial \xi^m} \overline{\hat{\varphi}(\xi)} e^{-i\alpha \xi} \Big|_{\xi=0} = 0, \quad (6.33)$$

and (see Lemma 2.2)

$$\overline{\hat{\varphi}(\xi)} e^{-i\alpha \xi} \Big|_{\xi=0} = 1, \quad (6.34)$$

for  $m = 1, 2, \dots, M$ .

Expanding  $\overline{\hat{\varphi}(\xi)} e^{-i\alpha \xi}$  in a Taylor series about  $\xi = 0$  gives according to (6.34) and (6.33)

$$\overline{\hat{\varphi}(\xi)} e^{-i\alpha \xi} = 1 + \frac{\xi^{M+1}}{(M+1)!} \frac{\partial^{M+1}}{\partial \xi^{M+1}} \overline{\hat{\varphi}(\xi)} e^{-i\alpha \xi} \Big|_{\xi=z}, \quad (6.35)$$

for some  $z \in (0, \xi)$ . Substituting (6.35) in (6.31) yields

$$s_l^{-j_0} = \frac{2^{j_0/2}}{2\pi} \int_{-\pi}^{\pi} \hat{u}(2^{j_0}\xi) e^{i\xi(l+\alpha)} d\xi + E_{M,j_0},$$

where

$$E_{M,j_0} = \frac{2^{j_0/2}}{2\pi} \int_{-\pi}^{\pi} \hat{u}(2^{j_0}\xi) e^{i\xi(l+\alpha)} \xi^{M+1} \frac{\partial^{M+1}}{\partial \xi^{M+1}} \left( \overline{\hat{\varphi}(\xi)} e^{-i\alpha\xi} \right) \Big|_{\xi=z} d\xi. \quad (6.36)$$

Clearly, the error  $E_{M,j_0}$  of the Taylor expansion is dependent on the choice of  $j_0$ .

It remains to compute  $(P_J u)^2$ ,  $(P_j u)(Q_j u)$ , and  $(Q_j u)^2$  in  $V_{j-j_0}$ . To this end, we define the reconstruction (representation) operators  $\mathcal{R}_v$  and  $\mathcal{R}_w$  respectively by

$$\begin{aligned} \mathcal{R}_v^{j,j_0} &: V_j \rightarrow V_{j-j_0}, \\ \mathcal{R}_w^{j,j_0} &: W_j \rightarrow V_{j-j_0}, \end{aligned}$$

We may then compute the projections

$$(P_{j-j_0} u)^2 = 2(\mathcal{R}_v^{j,j_0}(P_j u))(\mathcal{R}_w^{j,j_0}(Q_j u)) + (\mathcal{R}_w^{j,j_0}(Q_j u))^2, \quad (6.37)$$

for  $j = j_f, j_f + 1, \dots, J - 1$ , and on scale  $J$  we compute

$$(P_{j-j_0} u)^2 = (\mathcal{R}_v^{j,j_0}(P_J u))^2 + 2(\mathcal{R}_v^{j,j_0}(P_J u))(\mathcal{R}_w^{j,j_0}(Q_J u)) + (\mathcal{R}_w^{j,j_0}(Q_J u))^2. \quad (6.38)$$

We evaluate the right-hand sides of (6.37) and (6.38) in  $V_{j-j_0}$  to obtain the values of  $P_{j-j_0} u^2$ , and then project this result back into the wavelet basis, for  $j = j_f, j_f + 1, \dots, J$ .

For more a general analytic function  $f(u)$  we may apply the above procedure with the assumption that  $f(P_0 u) \in V_0$ , and use the 'telescopic' series

$$f(P_0 u) - f(P_J u) = \sum_{j=1}^J f(P_{j-1} u) - f(P_j u). \quad (6.39)$$

Using  $P_{j-1} = P_j + Q_j$  and the Taylor expansion for an analytic function gives

$$f(P_j u + Q_j u) = \sum_{n=0}^N \frac{f^{(n)}(P_j u)}{n!} (Q_j u)^n + E_{j,N}(f, u), \quad (6.40)$$

and hence

$$f(P_0 u) = f(P_J u) + \sum_{j=1}^J \sum_{n=0}^N \frac{f^{(n)}(P_j u)}{n!} (Q_j u)^n + E_{j,N}(f, u). \quad (6.41)$$

For a given accuracy  $\epsilon$  one can find  $N$  such that  $|E_{j,N}(f, u)| < \epsilon$ .

## 6.3 Numerical Results

We consider the heat equation given by

$$\begin{cases} u_t = \nu u_{xx} & 0 \leq x \leq 1, \\ u(0, t) = u(1, t) & 0 \leq t \leq 1, \end{cases} \quad (6.42)$$

for  $\nu > 0$ , with the initial condition

$$u(x, 0) = u_0(x) = \begin{cases} x, & 0 \leq x \leq 1/2, \\ 1 - x, & 1/2 \leq x \leq 1. \end{cases} \quad (6.43)$$

We solve the problem using the Crank-Nicolson scheme (see (4.11) Chapter 4) and the wavelet method described above with  $\nu = 1$ . As we can see in Figure 6.1, due to the irregularities at the points  $\{0, 1/2, 1\}$  in the initial condition, the Crank-Nicolson scheme generates a slow decay peak at these points rather than reproduce the smooth behaviour of the solution as seen in Figure 6.2 using wavelets (Daubechies wavelets of order 6).

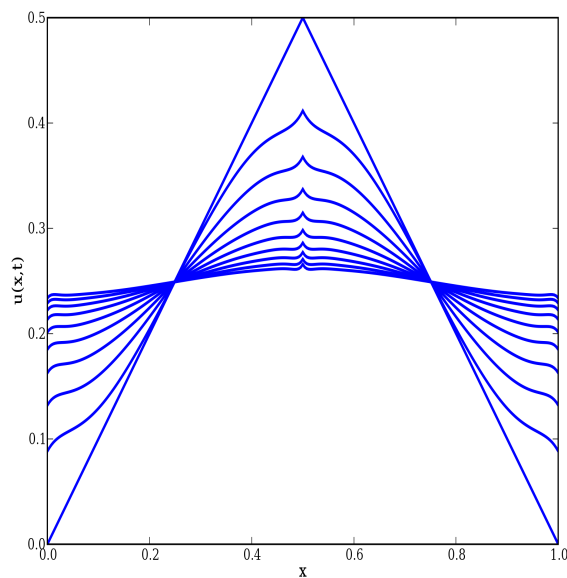


Figure 6.1: The solution of problem (6.42) with initial condition given in (6.43) computed using Crank-Nicolson scheme for several values of time  $t$  where  $\Delta t = 2^{-8}$

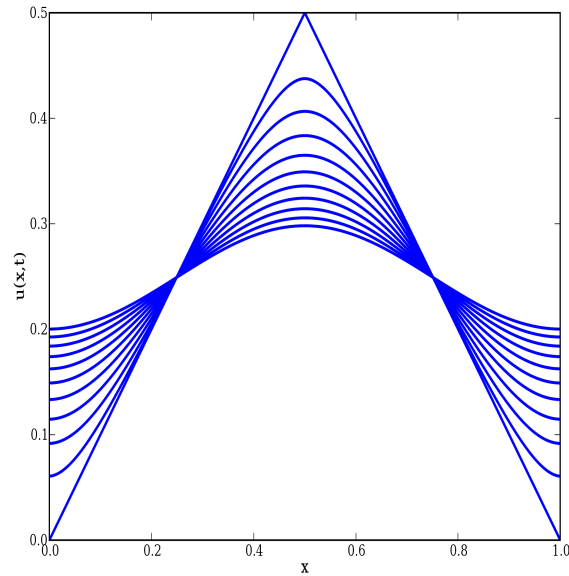


Figure 6.2: The solution of problem (6.42) with initial condition given in (6.43) computed in the wavelet domain for several values of time  $t$  where  $\Delta t = 2^{-8}$ .

We consider again problem (6.42) with initial condition given by

$$u(x, 0) = u_0(x) = \sin(2\pi x). \quad (6.44)$$

The exact solution of problem (6.42) and (6.44) is

$$u(x, t) = u_0(x)e^{-4\pi^2 t}. \quad (6.45)$$

The solution computed in the wavelet domain is shown in Figure 6.3.

We compare the norm-2 of the error for the Crank-Nicolson scheme in Figure 6.4(a) and the wavelet method in Figure 6.4(b).

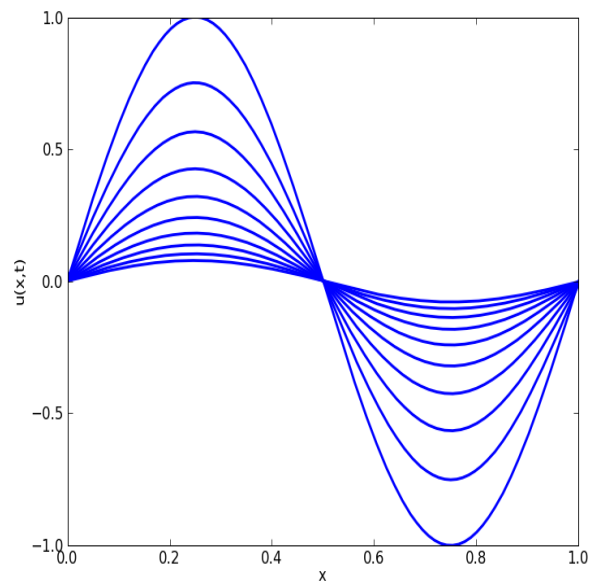
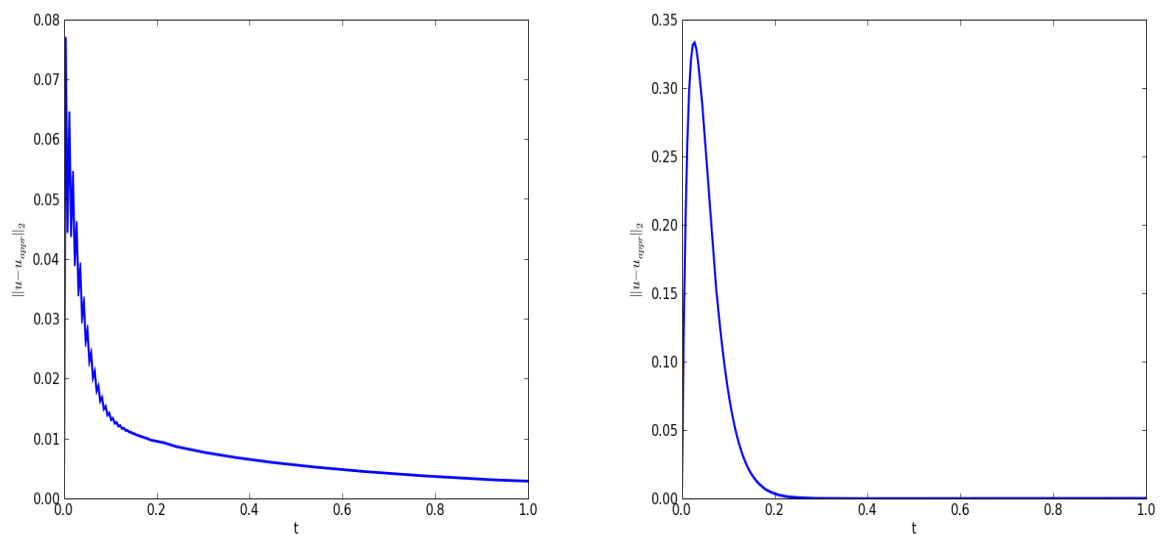


Figure 6.3: The solution of the problem (6.42) with  $u_0(x)$  given in (6.44) computed in the wavelet domain for several values of time  $t$  where  $\Delta t = 2^{-8}$ .



(a) Crank-Nicolson scheme

(b) The wavelet method

Figure 6.4: The norm-2 of the error.

We consider the Burger's equation given by

$$\begin{cases} u_t = \nu u_{xx} - uu_x & 0 \leq x \leq 1, \\ u(0, t) = u(1, t) & 0 \leq t \leq 1, \end{cases} \quad (6.46)$$

for  $\nu > 0$ , with the initial condition

$$u(x, 0) = u_0(x) = \sin(2\pi x). \quad (6.47)$$

We solve the non-linear problem (6.46) in the wavelet domain (see Figure 6.5), where  $\nu = 0.001$ ,  $\Delta t = 0.001$ ,  $n = 10$ ,  $J = 5$  and  $\epsilon = 10^{-6}$ . In Figure 6.5(a), the solution is computed from  $t = 0$  to  $t = 22/1000$ , and the initial condition is represented by red dash. The Gibbs phenomena is manifested in Figure 6.5(b), where the time interval is  $[0, 30/1000]$ .

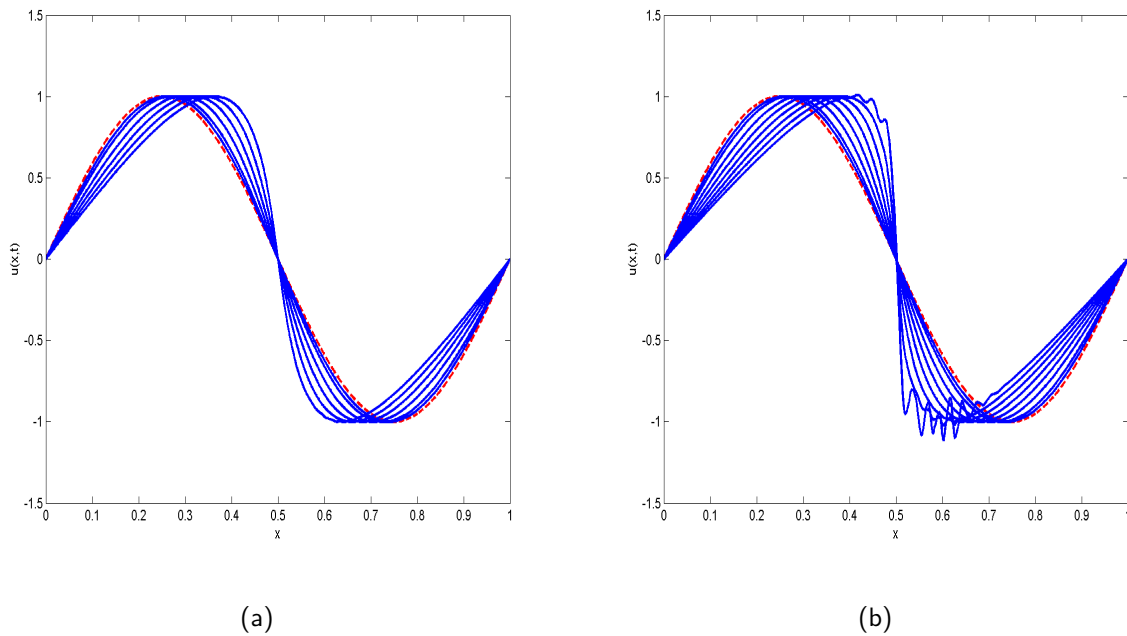


Figure 6.5: Solution of the problem (6.46) computed at every four time step.

## 7. Conclusion

In this thesis we have focused on the study of wavelets according to the following broad categories. We have given an overview of wavelet theory with emphasis on compactly supported wavelets, in particular the Haar wavelets and Daubechies wavelets. Thereafter, we have proceeded to the projection of some matrices and well-known operators using the standard form and the non-standard form.

Finally, we have discussed some application of wavelets to linear algebra and to differential equations. In linear algebra, our main interest is to use wavelet bases for solving sparse linear systems. We have shown that wavelet bases produce a well-conditioned system and also permit the numerical construction of the Green function, since it admits a sparse representation in this domain. Concerning differential equations, we have used wavelet bases to approximate the solution of differential equations by following two approaches which are the wavelet Galerkin method developed by Amaratunga *et al.* and the wavelet collocation discussed by Bertoluzza *et al.*, in which the autocorrelation functions generated by the scaling functions have been used to approximate the solution. In the wavelet Galerkin method, the authors have implemented their method only to equations of the Helmholtz type, but we have attempted to apply their method to equations of the form  $\mathcal{L}u = f$ , where  $\mathcal{L}$  is a linear differential operator. For the evolution equations, we have followed Beylkin *et al.*'s approach, where the differential equation is transformed to an integral equation so that we may represent the exponential operator in the wavelet domain.

For the future work, we will investigate the use of wavelets defined on the interval in the numerical solution of partial differential equations.

# Bibliography

- [1] S. Bertoluzza and G. Naldi. A wavelet collocation method for the numerical solution of partial differential equations. *Applied and Computational Harmonic Analysis*, 3:(9)1–9, January 1996.
- [2] G. Beylkin. On wavelet-based algorithms for solving differential equations. *In Wavelets: Mathematics and Applications*, pages 449–466.
- [3] G. Beylkin. On the representation of operators in bases of compactly supported wavelets. *SIAM J. Numer. Anal.*, 29(6):1716–1740, 1992.
- [4] G. Beylkin. Wavelet, multiresolution analysis and fast numerical algorithms. *ICASE Lecture notes*, 1993.
- [5] G. Beylkin. Wavelets and fast numerical algorithms. lecture notes for short course. *Proceedings for Symposia in Applied Mathematics*, 47, 1993.
- [6] G. Beylkin, R.R. Coifman, and V. Rokhlin. Wavelets in Numerical Analysis. *In Wavelets and Their Applications*, pages 181–210. Jones and Bartlett, 1992.
- [7] G. Beylkin and J. M. Keiser. On the adaptive numerical solution of nonlinear partial differential equations in wavelet bases. *J. Comp. Physics*, 132:233–259, 1997. PAM Report 262, 1995.
- [8] G. Beylkin and J.M. Keiser. An adaptive pseudo-wavelet approach for solving nonlinear partial differential equations. *In Multiscale Wavelet Methods for Partial Differential Equations*. Academic Press, 1997.
- [9] G. Beylkin, J.M. Keiser, and L. Vozovoi. A New Class of Stable Time Discretization Schemes for the Solution of Nonlinear PDEs. *Journal of Computational Physics*, 147(2). Academic Press, 1998.
- [10] B.E. Campbell. *On Wavelet Projection Methods for the Numerical Solution of Differential Equations*. Msc, University of Calgary, Alberta, Canada, 1999.



- 
- [11] C.K. Chui. *An Introduction to Wavelet Analysis*. Academy Press, Boston, 1992.
- [12] I. Daubechies, A. Cohen and P. Vial. Wavelets on the interval and fast wavelet transforms. *Appl. and Comp. Harmonic Anal.*, 1:54–81, 1993.
- [13] B. Alpert, G. Beylkin, R. Coifman and V. Rokhlin. Wavelet like bases for the fast solution of second kind integral equations. *SIAM J. Sci. Statist. Comput.*, 14(1):159–184, 1993.
- [14] G. Beylkin, R. Coifman and V. Rokhlin. Fast wavelet transforms and numerical algorithms 1. *Comm. Pure Appl. Math.*, 44:141–183, 1991.
- [15] W. Dahmen. Wavelet and multiscale methods for operator equations. *Acta Numerica*, 6:55–228, 1997.
- [16] I. Daubechies. *Ten Lectures on Wavelets*. Number 61 in CBMS-NSF series in Applied Mathematics. SIAM, Philadelphia, 1992.
- [17] M. Dorobantu. *Wavelet-based Algorithms for fast PDE Solvers*. Phd, Royal Institute of Technology, Stockholm, Sweden, 1995.
- [18] L. Greengard and V. Rokhlin. On the Numerical Solution of Two-Point Boundary Value Problems. *Comm. Pure Appl. Math.*, 44(4):419, 1991. Yale University Technical Report, YALEU/DCS/RR-692 (1989).
- [19] S. Jaffard. Wavelet methods for fast resolution fo elliptic problems. *SIAM J. Numer. Anal.*, 29(4):965–986, 1992.
- [20] J.L. Journé. *Calderón-Zygmund Operators, Pseudo-differential operators and the Cauchy Integral of Caldereón*. Number 994 in Lecture Notes in Mathematics. Springer-Verlag, Berlin, 1983.
- [21] J.M. Keiser. *On I. Wavelet Based Approach to Numerical Solution of Nonlinear Partial Differential Equations and II. Nonlinear Waves in Fully Discrete Dynamical Systems*. PhD thesis, University of Colorado at Boulder, 1995.
- [22] S. Mallat. Multiresolution approximation and wavelets. *Trans. Amer. Math. Soc.*, 315:69–88, 1989.

- [23] S. Mallat. A theory for multiresolution signal decomposition: the wavelet representation. *IEEE Trans. PAMI*, 11:674–693, 1989.
- [24] Y. Meyer. *Ondelette et operateurs*. Hermann, 1990.
- [25] Y. Meyer. Ondelettes sur l'intervalle. *Revista Matemática Iberoamericana*, 7(2):115–133, 1991.
- [26] J.H. Bramble, J.E. Pasciak and J. Xu. Parallel multilevel preconditioners. *Math. Comput.*, 55(191):1–22, 1990.
- [27] A. Pazy. *Semigroups of Linear Operators and Applications to Partial Differential Equations*. Springer-Verlag, 1983.
- [28] W. Proskurowski and O. Widlund. On the numerical solution of Helmholtz's equation by the capacitance matrix method. *Mat. Comp.*, 30(135):433–468, 1976.
- [29] K. Amaratunga, J.R. Williams, S. Qian and J. Weiss. Wavelet-galerkin solutions for one-dimensional partial differential equations. *International Journal for Numerical Methods in Engineering*, 37, 1994.
- [30] M. Rasajski. Preconditioning in a wavelet basis and its application to some boundary problems. pages 64–85. Pub.Elektrotehn. Fak., Univ. Beograd, Ser. Mat. (14)2003.
- [31] A. Latto, H.L. Resnikoff and E. Tenenbaum. The evaluation of connection coefficients of compactly supported wavelets. In *Proceedings of the French-USA. Workshop on Wavelets and Turbulence*. Springer-Verlag, 1992, Princeton Univ, June 1991.
- [32] R.L. Schult and H.W. Wyld. Using wavelets to solve the burgers equation: A comparative study. *Phys. Rev. A*, 46(12):7953–7958, Dec 1992.